UNIVERSITY OF TRENTO

DEPARTMENT OF PHYSICS

UNDERGRADUATE DEGREE IN PHYSICS

Tidal Deformation of Neutron Stars

Supervisor
Prof. Albino Perego

Candidate
Zenari Marco
209392

Academic Year 2021-2022

Acknowledgements

I would like to thank my supervisor and professor Albino Perego for his availability and for providing guidance and feedback throughout the work on this thesis.
I would also like to thank my family and my friends Claudia, Leonardo and Stefano for their support in the achievement of this result.

Contents

Chapter 1

Introduction

An important prediction of general relativity (GR) is the emission of gravitational waves (GWs), ripples in the curvature of space-time, by a system with a time-varying quadrupole moment, such as a binary system composed of two neutron stars (BNS). Efforts to directly prove the existence of GWs have been done for more than fifty years, as the waves are so tiny that their detection requires highly sensitivity detectors, as long-arm interferometers. For this reason, Einstein himself doubted that they could ever be detected. The remarkable accomplishment of their detection was made by the LIGO collaboration (GW150914), in September 2015. Nowadays, tens of detections have been reported. The detection of a BNS merger, GW170817, on 17 August 2017 had a profound impact in our understanding of gravity and the physics of dense matter. It has indeed provided a large amount of data that opened up the possibility to explore matter under extreme conditions, in regimes that would be inaccessible by experiments on earth. In particular, gravitational waves from the inspiral phase of binary neutron stars mergers can be used to measure the tidal deformability of the stars, setting stringent constraints on the equation of state (EOS) of cold ($T = 0$) nuclear matter. Also the post-merger gravitational waves signal and the associated electromagnetic signature could provide unique information on the EOS of hot ($T \geq 10\,\mathrm{MeV}/k_\mathrm{B}$) and dense ($n \geq n_0$) stellar matter, where $n_0 = 0.16\,\mathrm{fm}^{-3}$ is the nuclear saturation density.

The aim of this thesis is to study the main aspects of neutron stars (NSs) and neutron star binary systems. We will focus in particular on the tidal effects on a neutron star in the final moments of the inspiral, described through the Love number k_2 which is the object of our computational calculation.
In chapter 2 we will start from the history of neutron star discovery, happened thanks to the detection of pulsars. We will briefly discuss their origins in supernovae (SN) and their observational properties. We will introduce a simple model, the magnetic dipole model, to describe the spin down of a pulsar. At the end of the chapter we will discuss the equations that are needed to describe the stars both in Newtonian gravity and in general relativity, where the Tolman-Oppenheimer-Volkoff (TOV) equations play a fundamental role in the determination of the structure of the stars.
The microscopic aspects of neutron stars will be covered in chapter 3, where some models of equation of state of NS matter will be introduced. The first and simple model will be the non-interacting fermions gas that, although been simple and analytical, does not produce realistic results in astrophysical models. The problems of such a model will be identified and a more realistic equation of state, the Bombaci-Logoteta [3], [8] equation of state (BL EOS), will be introduced. Such equation of state is the one used in the code that will be presented in chapter 6.
In chapter 4 we will discuss binary systems, starting from their dynamical evolution in Newtonian gravity described by Kepler's laws and then studying the effects of gravitational waves emission in general relativity. We will than briefly discuss the accretion mechanism occurring during the evolution of two regular stars forming a compact binary system, before focusing on the particular case of double neutron star systems. The archetype of such systems is the Hulse-Taylor binary, that has been discovered in 1974 and its evolution has been observed for more than 30 years. This system has been a perfect gravitational

laboratory, being in excellent agreement with the general relativity predictions.
In chapter 5, the main topics of this thesis will be presented: the tidal deformation of neutron stars. In first place we will introduce tidal forces in Newtonian gravity, taking the Earth-Moon system as example and deriving the classical relation for tidal forces $\propto GM/r^3$. Then we will introduce the equations that describe tidal effects in general relativity, without discussing too deeply their derivation. At the end of chapter 5 the theory of Love numbers will be covered and in particular we will explain the equations that lead to the calculation of the Love number k_2.
In chapter 6 we will explain the numerical method used to integrate the TOV equations together with the Love number equations, and we will present our results, that are compatible with the results obtained by the public code described in ref. [2] and [6].
The references used for each chapter are cited in its introduction and more specific citation will appear in the figures credits and in the parts where particular results are derived. Some other references that has been consulted are [16], [9] and [1].

Chapter 2

Neutron stars

In this chapter we will introduce the main aspects of neutron stars following ref. [15] and focusing mainly on their observational properties. A brief discussion about their origins in supernovae explosions and their discovery by the scientific community will also be presented. At the end of the chapter we will present a simple model to describe the spin down of pulsars, the magnetic dipole model.

2.1 Supernovae

Supernovae are powerful and luminous explosions of stars. They are named by the abbreviation SN followed by the year of discovery and a letter which indicates the alphabetically order in which they were discovered. Supernovae are rare in our Galaxy, and occur every 30-50 years. Supernovae produce the

Figure 2.1: Picture of the SN 1994D taken by the Hubble Space Telescope. Credits: NASA, ESA, The Hubble Key Project Team, and The High-Z Supernova Search Team.

bulk of heavy elements in the Universe and disperse them throughout the interstellar medium. Most of the oxygen, calcium and silicon are produced in these catastrophic explosions. They are also important for the formation of new stars in two ways: directly by forming neutron stars and black holes and indi-

rectly by pumping an energy of about 10^{51} erg into their host galaxy triggering the collapse of molecular clouds in new stars. Highly relativistic particles are also produced by supernovae forming the so called cosmic rays.
Supernovae classification is based on their spectra near maximum light and distinguishes between two types: Type I and Type II. The principal difference between Type I and Type II is the presence of hydrogen lines in their spectra. Hydrogen lines are present in Type II supernovae but are absent in Type I. Type II can be classified further by the shape of their light curves which is the evolution of the light intensity as function of time. Type I are also categorized further based on the presence of certain silicon lines and possibly helium lines in their spectra. Type II supernovae and some classes of Type I (e.g. Type Ib and Type Ic) are caused by the collapse of the iron core of massive stars ($M > 8M_{\odot}$). During the collapse protons in the core capture electrons forming neutrons and emitting neutrinos. This process leaves a remnant behind which gives birth to neutron stars or black holes of a few solar masses.

2.2 History of neutron stars discovery

The idea that core-collapse supernovae could produce compact stars made of neutrons was introduced by Walter Baade and Fritz Zwicky in 1934. The solution of the general relativistic stellar structure equations for a pure neutron gas led Oppenheimer and Volkoff to the interior structure of a neutron star in 1939. The observational discovery of neutron stars had to wait until 1967, when a group of researcher of the Cavendish Laboratory in Cambridge discovered a series of regular pulses of 1.3 s period, which is too short to come from the oscillation of a star. The first clue was that it may have been a terrestrial signal. After making sure that they were picking up the signal from outside the Solar System it became a discussed explanation that the signal had been sent by another civilization in our Galaxy. For this reason, the source was initially named LGM which stands for little green men. After some time, more of these pulsing radio sources were found and the explanation in terms of signals produced by an other civilization became more and more unlikely. This type of sources of radio signals were called *pulsars*. Thomas Gold and Franco Pacini proposed the explanation that pulsars are highly magnetized, rotating neutron stars. In section 2.5 a model based on this idea will be discussed.

2.3 Observational properties

Pulsars are usually discovered by identifying a periodic signal hidden in the noisy time series collected by radio telescopes. As shown in figure 2.2 they populate mainly the disk of our Galaxy but some are found at very high latitudes. We can estimate their distance from us using an effect called *pulse dispersion*. The emitted pulse is spread over a finite frequency range. The high frequencies travel with a larger group velocity through the interstellar medium and therefore they arrive earlier at the radio telescope. The time delay between high and low frequencies detection can be expressed as

$$\Delta t = 4150\text{s} \left(\frac{1}{\nu_{low}^2} - \frac{1}{\nu_{high}^2} \right) DM, \tag{2.1}$$

where $DM$is the *dispersion measure*, defined as

$$DM = \int_0^d n_e(x)\mathrm{d}x. \tag{2.2}$$

In equation 2.2 d is the distance to the pulsar and n_e is the number density of free electrons in the interstellar medium along the line that connect the pulsar to the telescope. To infer d a model of the free electrons distribution in the Galaxy is needed. Such model can be tested with pulsar whose distance is known via other methods, such as trigonometric parallax.

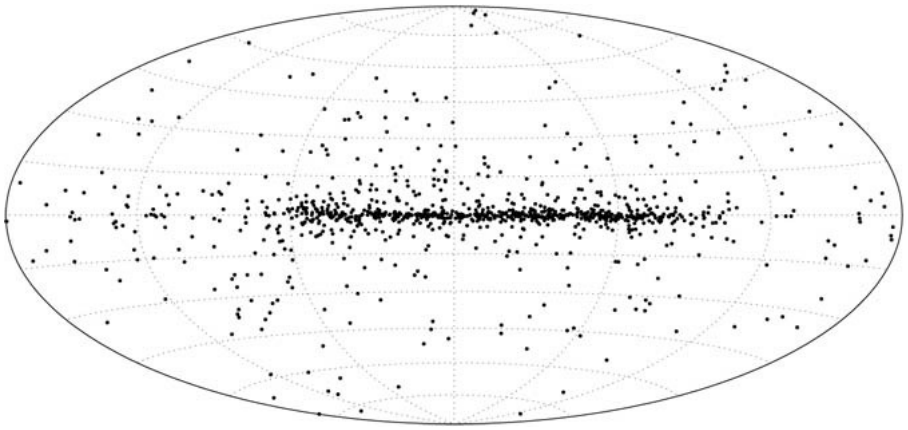

Figure 2.2: Distribution of 1026 pulsars in the Galaxy in Galactic coordinates. The central line refers to the Galactic plane. Credits: [10]

Angular momentum conservation in a collapsing star causes a huge increase in spin of the collapse product. Moreover, matter accretion from a companion star can also spin up a NS. For these reasons neutron stars rotate rapidly with rotation periods between 1.5 ms and several seconds. Pulsars are generally good clocks, although they spin down very slowly causing a change in the period. In figure 2.3 there is a plot of observed pulsar $P - \dot{P}$ where P is the period and $\dot{P}$ is the absolute value of its time derivative. Evidently pulsars can be divided in two classes: normal pulsars have a rotation period of 0.1 to 1 s and spin down at a rate of 10^{-15} ss^{-1} while millisecond pulsars' period is between 1.5 and 30 ms and become slower at a rate of 10^{-19} ss^{-1}. Many aspects of the pulsars can be interpreted using the magnetic dipole model, that will be discussed in section 2.5. The main assumption in this model is that the observed slowdown of a pulsar is due to the emission of magnetic dipole radiation. Two important predictions of this model are:

- the spin-down is related to the magnetic field: $\dot{P} \propto B^2$;
- the magnetic field strength can be deduced from P and $\dot{P}$: $B \propto \sqrt{P\dot{P}}$.

The consequences of this model are that young pulsars, with a large magnetic fields, spin down rapidly while millisecond pulsars, that are found mainly in binary systems, spin down very slowly.
Another interesting observational fact about pulsars is that they are often found having large velocities in the galaxy, some as high as 1000 km s^{-1}, and known as *kick velocities*. These velocities are much higher than the velocities of their progenitor stars, which typically have velocities of 10 to 50 km s^{-1}. The reason for these large velocities is that even a very small asymmetry in the core-collapse process imparts a kick velocity of several 100 km s^{-1} to the new born neutron star.
In general it may be very difficult to measure the mass of an isolated star. Luckily, about one half of the stars are members of binary systems so we can measure at least the total mass of the system. Among pulsars, only 4% are members of a binary system, probably because of the violent neutron-star formation process. If the five Keplerian parameters and two more post Newtonian parameters are known (in case of important general relativistic effects), the mass of the individual star can be determined. Generally pulsar masses are close to 1.35 $M_\odot$. An upper bound for the mass of neutron stars is object of theoretically discussion: the *degeneracy pressure* contrasts the gravitational collapse up to a maximum point, which is not exactly known. If the mass exceeds that limit the gravitational collapse causes the formation of a black hole. Type II supernovae produce neutron stars with masses close to the observed 1.35 $M_\odot$. Other astrophysical processes such as accretion from a companion star can increase the mass of a neutron star.

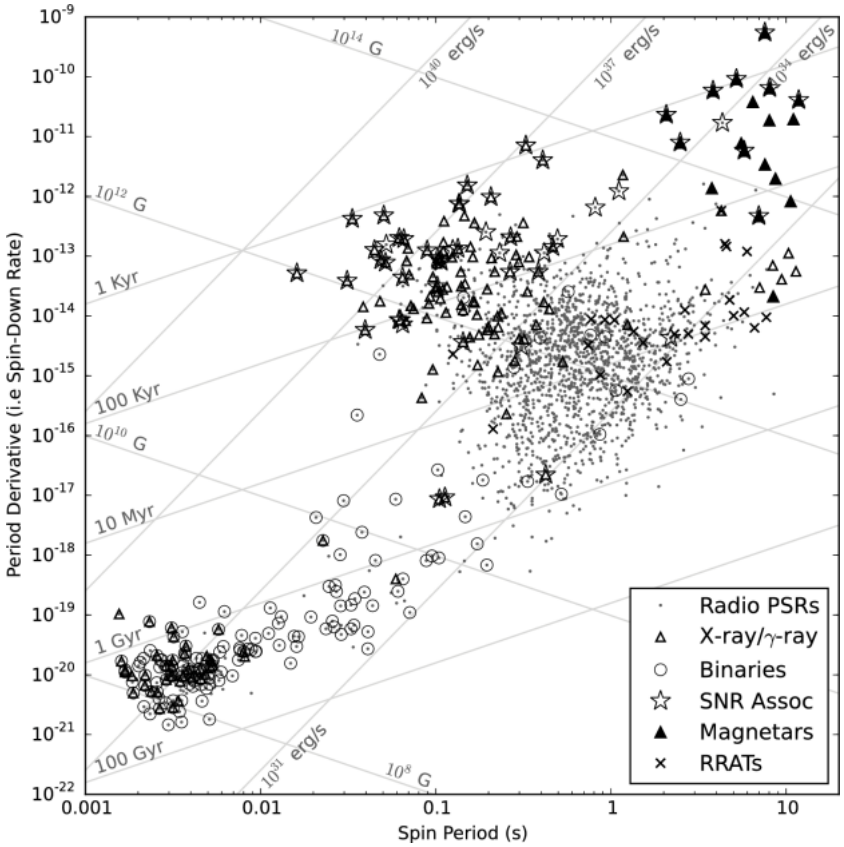

Figure 2.3: $P - \dot{P}$ diagram for a sample of radio pulsar. In the legend different type of pulsars are identified, including the ones being part of a binary system. Credits: [5] chapter 6.

2.4 Pulsars

As anticipated there is a general consensus that pulsars are indeed rotating neutron stars. This hypothesis is based on three pulsars properties:

- they have short periods down to 1.5 ms;
- their periods increase with a rate of $\dot{P} \sim 10^{-15}$ ss^{-1} ;
- they emit a very regular signal.

From causality arguments we can obtain a maximum radius for a source of period τ. Such radius should be smaller than the light-travel distance $D < c\tau$. By inserting $\tau = 1.5$ms we obtain a maximum radius of about 450 km. White dwarfs of 1.35 $M_\odot$ have a radius of 3000 km, therefore pulsars can only be neutron stars or black holes. It is also difficult to assert any radiation entity to a black hole, so the objects behind pulsars have to be neutron stars. The remaining question is if the neutron star pulsates or rotates. In case of pulsation the oscillation period is of the order of the dynamical time scale, which is given by

$$\tau_{\text{osc}} \approx \tau_{\text{dyn}} = \sqrt{\frac{1}{G\langle\rho\rangle}}, \tag{2.3}$$

where $\langle\rho\rangle$ is the average density of the star. The problem is that using the measured $\tau = 1.5$ ms we obtain a density of $\langle\rho\rangle = 7 \cdot 10^{12}$ g cm^{-3} which is two orders of magnitude less than the average density of neutrons stars. We expect indeed an average density of 10^{15} g cm^{-3} which is the average density for

an object of mass 1.4 $M_\odot$ and radius 10 km. Let's now consider the rotation hypothesis. The maximum rotation frequency can be determined equaling the centrifugal force on a mass element at the stellar surface to the gravitational attraction from the star (for rigid rotation). Obviously this gives us an upper limit for the rotation frequency that leads us to a lower limit to the average density. We obtain:

$$\omega^2 = G\frac{M}{R^3} = G\frac{4}{3}\pi\langle\rho\rangle, \tag{2.4}$$

or

$$\langle\rho\rangle = \frac{3\pi}{GP^2}, \tag{2.5}$$

where we have substituted the period P to the frequency ω as $\omega = 2\pi/P$. Inserting a period $P = 1.5\,\mathrm{ms}$ we obtain an average density of about $6 \cdot 10^{13}\,\mathrm{g\,cm^{-3}}$, which is closer to a real neutron star density (considering that it is a lower limit). The fact that pulsars rotation slows down is also in agreement with the idea that pulsars are rotating neutron stars.

2.5 The magnetic dipole model

The magnetic dipole model is a simple model of a pulsar which explains many of the observational properties. The assumption is that a pulsar is a rigid, magnetized sphere that rotates in vacuum, with a magnetic moment $\vec{m}$ and a dipolar magnetic field. If we call α the angle between the rotation axis and the magnetic moment, the dipolar magnetic field is given by

$$\vec{B}(\vec{r}) = \frac{3\vec{n}(\vec{m}\cdot\vec{n}) - \vec{m}}{r^3}, \tag{2.6}$$

where $r = |\vec{r}|$ and $\vec{n} = \vec{r}/r$. This formula can be used to determine the magnetic field at the pole, using $\vec{m} \parallel \vec{n}$ and $r = R$ where R is the radius of the star,

$$\vec{B}_p = 2\frac{\vec{m}}{R^3}. \tag{2.7}$$

Inverting the equation we obtain

$$\vec{m} = \frac{\vec{B}_p R^3}{2}. \tag{2.8}$$

A time-varying magnetic dipole radiates a power

$$\left(\frac{dW}{dt}\right) = -\frac{2}{3c^3}|\ddot{\vec{m}}|^2. \tag{2.9}$$

The second time derivative of the dipole moment can be obtained considering that $\vec{m}$ forms an angle α with the rotation axis, that we can assume being the z-axis of our coordinate system. Therefore $\vec{m} = m_0\hat{e}_m$ where $m_0 = B_p R^3/2$ and $\hat{e}_m = (\sin\alpha\cos\omega t, \sin\alpha\sin\omega t, \cos\alpha)$ where ω is the angular frequency at which $\vec{m}$ rotates. Deriving with respect to the time twice we obtain

$$|\ddot{\vec{m}}|^2 = m_0^2\omega^4\sin\alpha^2, \tag{2.10}$$

and the total emitted power is

$$\left(\frac{dW}{dt}\right) = -\frac{B_p^2 R^6}{6c^3}\omega^4\sin\alpha^2. \tag{2.11}$$

If we assume that the emitted energy is tapped from the rotational energy of the pulsar

$$E_{rot} = \frac{1}{2}I\omega^2, \tag{2.12}$$

where I is the moment of inertia, then deriving with respect to time we obtain

$$\frac{dE_{rot}}{dt} = I\omega\dot{\omega}. \tag{2.13}$$

Equating dE_{rot}/dt and dW/dt and solving for $\dot{\omega}$ we obtain

$$\dot{\omega} = -\frac{B_p^2 R^6 \omega^3 \sin\alpha^2}{6c^3 I}, \tag{2.14}$$

and as expected the pulsar slows down.

2.6 Stellar structure equations

The structure of a neutron star is much more complex than the structure of other stars, which are in general determined by *hydrostatic equilibrium*, the equilibrium between gravity and the pressure forces that are the result of the microscopic interactions in the stellar material. Gravity inside and at the surface of NSs is so strong that general relativity is necessary to describe them and for this reason one has to consider the relativistic generalization of the stellar structure equations, the *Tolman-Oppenheimer-Volkoff* equations. In neutron stars the separations between nucleons is comparable to their size and for this reason in order to elaborate a model to describe realistically neutron stars one needs to consider all the fundamental interactions. The equations of stellar structure for ordinary stars are in general:

- an equation that relates the density to the mass (mass equation);
- an equation for the hydrostatic equilibrium;
- an equation for the gravitational potential;
- an equation that relates nuclear energy to the luminosity;
- a radiative diffusion equation;

In this section we will study the first three equations in Newtonian gravity and assuming spherical symmetry. After that, we will consider their corrections in general relativity. For NSs, temperature is assumed to be 0, while the pressure gradient is just provided by degeneracy and not by nuclear energy. Thus, the last two equations will be neglected.

2.6.1 Newtonian case

We imagine the star as made up of infinitesimally thin, homogeneous shells, at radius r with a width of dr. The mass equation can be found using the definition of density:

$$dm = 4\pi r^2 \rho dr, \tag{2.15}$$

or

$$\frac{dm(r)}{dr} = 4\pi r^2 \rho(r). \tag{2.16}$$

The mass density ρ is related to the energy density $\varepsilon = \rho c^2$. Equation 2.16 becomes

$$\frac{dm(r)}{dr} = \frac{4\pi r^2 \varepsilon(r)}{c^2}. \tag{2.17}$$

The total mass of the star can be found by integration from the center to the radius R of the star, which is defined as the location where the pressure vanishes. The hydrostatic equilibrium equation expresses the equilibrium between gravity and pressure. The net force per area is given by

$$P(r) - P(r+dr) = -\frac{dP}{dr}dr, \tag{2.18}$$

where $P(r)$ is the pressure at a distance r from the center and the minus sign appears because the pressure decreases going outward. The gravitational force on the shell of radius r is determined by the mass enclosed in the shell and it is given by

$$f_{grav} = \frac{Gm(r)}{r^2}\rho 4\pi r^2 dr. \tag{2.19}$$

Equating the gravitational force and the force per area we obtain the second star structure equation

$$\frac{dP}{dr} = -\frac{Gm(r)}{r^2}\rho. \tag{2.20}$$

The equation for the gravitational potential is given by Newtonian gravity theory

$$\frac{d\Phi}{dr} = \frac{Gm(r)}{r^2}. \tag{2.21}$$

2.6.2 The Tolman-Oppenheimer-Volkoff equations

The generalization of the equations illustrated in the previous section is due to Tolman, Oppenheimer and Volkoff. A derivation of the generalized equation can be found in ref. [14] by Misner, Thorne and Wheeler. The *TOV equations* can be written in a form which puts in evidence the correction factors to the Newtonian ones.

$$\frac{dm}{dr} = \frac{4\pi r^2 \varepsilon}{c^2}, \tag{2.22}$$

$$\frac{dP}{dr} = -\frac{G\varepsilon m(r)}{c^2 r^2}\left(1+\frac{P}{\varepsilon}\right)\left[1+\frac{4\pi r^3 P}{m(r)c^2}\right]\left[1-\frac{2Gm(r)}{c^2 r}\right]^{-1}, \tag{2.23}$$

$$\frac{d\Phi}{dr} = -\frac{c^2}{\varepsilon}\frac{dP}{dr}\left(1+\frac{P}{\varepsilon}\right)^{-1}. \tag{2.24}$$

The equation for the mass appears as the same as the Newtonian one, but here ε is the total energy density which contains all forms of energy. The equation for the pressure has three corrections: the first two are special relativistic corrections while the third one is due to general relativity. This last correction provides us with a criterion to understand if GR is important and has to be accounted for. If the following condition holds

$$\xi = \frac{2GM}{c^2 R} \ll 1, \tag{2.25}$$

the GR corrections are not important. We note here that the quantity $r_S = 2GM/c^2$ has the dimensions of a length and is generally referred to as *Schwarzschild radius*. For a typical white dwarf of $0.6\mathrm{M}_\odot$ and a radius of about 10^4 km, ξ is approximately $1.8\cdot 10^{-4}$ and therefore GR corrections can be neglected. For a NS with $1.4\,\mathrm{M}_\odot$ and 10 km radius, $\xi \approx 0.4$ and therefore general relativistic effects are important. The integration of equation 2.22 yields the gravitational mass M_{grav}. This quantity is different from the baryonic mass defined as the sum of all the baryons in the star $M_{\mathrm{bar}} = Nm_{\mathrm{bar}}$, where m_{bar} is the mass of the single baryon and N the total number of baryons. The difference is due to the gravitational binding energy B that is the energy that is needed to disperse all the baryons of the star to infinity. The two masses are related through the binding energy as $M_{\mathrm{bar}} = M_{\mathrm{grav}} + |B|/c^2$. Typically the binding energy of

a neutron star is about $0.2\,M_{\odot}c^2$.
Using TOV equations instead of Newtonian equations in numerical simulation and confronting the results leads to the intuition that gravity is stronger in GR than in Newtonian gravity. This is due to the fact that in Newtonian gravity mass is the only source of gravity, while in GR space-time curvature is due to all components of the momentum-energy tensor. So, all forms of energy, including pressure, contribute to gravity.

Chapter 3

Equation of state of a neutron star

In chapter 2 we have discussed the equations that rule the macroscopic structure of neutron stars. In this section we will discuss how pressure is related to energy density and we will find the microscopic equation of state of neutron stars. In the following section we will follow ref. [15] in presenting the equation of state of a non-interacting, ideal Fermi gas proposed for the first time by Tolman, Oppenheimer and Volkoff in 1939. They obtained a neutron star radius of about 10 km, not far away from modern results, but a maximum mass of only 0.7 $M_\odot$. In the second part of the chapter we will discuss effects that are not included in this simplified treatment and we will follow ref. [8] in presenting the BL equation of state.

3.1 Non-interacting fermions

Let's assume that the neutron star is made entirely out of neutrons, even though we know that this is not entirely true. In fact some neutrons will indeed decay via $n \to p + e + \bar{\nu}_e$ and the neutrinos will escape, until a sufficiently large number of electrons has been built up. Electrons are fermions and obey the Pauli exclusion principle, therefore they cannot occupy the same state. For this reason, only a limited number of electrons can have the same energy (the ones with different spin). If more and more electrons are produced they have to occupy higher and higher energy levels. At some point, the newly produced electrons will not have a large enough energy to occupy the free high-energy levels. The decay process will then stop and this suppression is referred as *Pauli blocking*.
In this model we consider only neutrons and we assume that the pressure is provided only by them (in white dwarf the pressure is provided by electrons). The neutrons obey the Fermi-Dirac distribution

$$f(E) = \frac{1}{\exp\left[\frac{(E-\mu)}{k_B T}\right] + 1}, \tag{3.1}$$

where E is the energy level of the particle, μ is the chemical potential, k_B is the Boltzmann constant and T is the gas temperature. By integration of the distribution function we can derive the number density n, the pressure P and the energy density ε of the system. In the model we consider only $T = 0$, which is a good approximation because to be comparable with the typical Fermi energies in a neutron star of $1\,\mathrm{MeV}$ we need a temperature of about $T = 1\,\mathrm{MeV}/k_B = 10^{10}\,\mathrm{K}$, which is much larger than the surface temperature of observed NSs.
With $T = 0$ the distribution function becomes a step function that vanishes beyond the Fermi momentum

$$p_F = \left(\frac{3h^3}{8\pi} n\right)^{1/3}. \tag{3.2}$$

We can write the number density as function of the Fermi momentum

$$n = \frac{8\pi}{h^3}\int_0^{p_F} p^2 dp = \frac{8\pi}{3h^3}p_F^3. \tag{3.3}$$

The energy that corresponds to this momentum is called Fermi energy:

$$E_F = \sqrt{p_F^2c^2 + m^2c^4}. \tag{3.4}$$

The energy density is given by

$$\varepsilon(p_F) = \int E dn = \frac{8\pi}{h^3}\int_0^{p_F} \sqrt{p^2c^2 + m^2c^4}\, p^2 dp \tag{3.5}$$

$$\varepsilon(p_F) = \frac{8\pi}{h^3}m^4c^5\int_0^{p_F/mc} \sqrt{1+z^2}\, z^2 dz \tag{3.6}$$

$$\varepsilon(p_F) = \varepsilon_0\left[\sqrt{1+x^2}\left(x+2x^3\right) - \sinh^{-1}x\right], \tag{3.7}$$

where we have substituted $z = pc/mc^2$ and defined $x = p_F/mc$ the dimensionless momentum and the quantity $\varepsilon_0 = \pi m^4c^5/h^3$ that has the dimensions of energy per volume.
Now that we know the energy density we can use the thermodynamics equations

$$P = -\left.\frac{\partial(\varepsilon/n)}{\partial(1/n)}\right|_{s,Y_I}, \tag{3.8}$$

for the pressure,

$$T = \left.\frac{\partial(\varepsilon/n)}{\partial s}\right|_{n,Y_I}, \tag{3.9}$$

for the temperature and

$$\bar{\mu}_i = \left.\frac{\partial(\varepsilon/n)}{\partial Y_i}\right|_{n,s} = \left.\frac{\partial\varepsilon}{\partial n_i}\right|_{n,s}, \tag{3.10}$$

where $Y_i = n_i/n$ is the abundance of a species i, for the chemical potential. Note that with the bar is denoted the chemical potential that includes the rest mass. The chemical potential without the rest mass is indicated with $\mu_i = \bar{\mu}_i - m_ic^2$. The chemical potential is the energy required to add a new particle to the system. In our case ($T = 0$) $\bar{\mu}_i$ corresponds to the Fermi energy.
In a similar way as done for the energy density we can calculate the pressure. However we need to express the velocity in terms of energy and momentum using the relativistic relation $v = pc^2/E$. Therefore

$$\begin{aligned} P(p_F) &= \frac{1}{3}\int_0^{p_F} pv\frac{8\pi p^2 dp}{h^3} = \\ &= \frac{8\pi c^2}{3h^3}\int_0^{p_F}\frac{\pi p^4 dp}{(p^2c^2+m^2c^4)^{1/2}} = \\ &= \frac{\varepsilon_0}{3}\int_0^{p_F/mc}\frac{z^4 dz}{\sqrt{1+z^2}} = \\ &= \frac{\varepsilon_0}{24}\left[\left(2x^3-3x\right)\sqrt{1+x^2} + 3\sinh^{-1}x\right], \end{aligned} \tag{3.11}$$

where ε_0 and x are defined as before.
Equations 3.7 and 3.11 are not immediate to interpret and it is therefore useful to consider the non-relativistic and the ultra-relativistic limits. For the non-relativistic limit we can use $v = p/m$ and the pressure results in

$$P = \frac{8\pi}{15h^3m}p_F^5. \tag{3.12}$$

If we insert equation 3.2 we obtain that $P \propto \rho^{\frac{5}{3}}$. An equation of state of the form $P = K\rho^{\Gamma}$ is called *polytrope* and Γ is called polytropic exponent. In the ultra-relativistic limit we can put $v = c$ and the pressure becomes

$$P = \frac{8\pi c}{3h^3}\int_0^{p_F} p^3 dp = \frac{2\pi c}{3h^3}p_F^4, \tag{3.13}$$

and using $p_F \propto n^{1/3}$ we have $P \propto \rho^{4/3}$.
For an ideal neutron star we can construct a model by solving equations 2.22, 2.23 and 3.11.
Unfortunately, as anticipated before, the idea that in a neutron star there are only neutrons is basically incorrect because a small fraction of neutrons decay forming electrons and protons. At the equilibrium (β *equilibrium*) the reaction of decay

$$n \to p + e + \bar{\nu}_e, \tag{3.14}$$

and the electric capture reaction

$$e + p \to n + \nu_e, \tag{3.15}$$

have to be equally fast. Knowing that the neutrinos escape the β-equilibrium condition for the chemical potentials is

$$\bar{\mu}_n = \bar{\mu}_p + \bar{\mu}_e, \tag{3.16}$$

where the mass energies are included $\bar{\mu}_i = \mu_i + m_i c^2$.
If we have a mixture of Fermi gases, as in this case made of neutrons, protons and electrons, the total energy density and pressure are given by the sum of the constituents:

$$\varepsilon = \sum_{i=e,p,n} \varepsilon_i, \tag{3.17}$$

$$P = \sum_{i=e,p,n} P_i. \tag{3.18}$$

This is a slightly correction to the previous model that includes the effects of the neutron decay.

3.2 More realistic equations of state

In the previous section we have neglected the interaction between nucleons in a neutron star. In a typical neutron star with a mass of $1.4\,M_\odot$ the number of nucleons is approximately $1.7 \cdot 10^{57}$, which means for a star with a 12 km radius that the typical distance between the nucleons is about 1 fm. From scattering experiments we know that a nucleon has approximately a radius of 0.8 fm which means that nucleons are practically touching each other. For this reason, their interaction in a neutron star cannot be ignored. If this interaction is taken into account, the resulting neutron star can be much more massive than the one discussed in section 3.1.
In this section we briefly introduce the main matter constituents of neutron stars. The lightest particles are the *leptons*, spin 1/2 fermions that do not experience nuclear force. The leptons are divided in three flavors with two particles each: electron and electron-neutrino, muon and μ-neutrino, tau and τ-neutrino. The masses of the neutrinos are not known exactly, but very small (less than 2 eV). For each of these particles there exists an antiparticle. Other than leptons, we have *baryons*, which are fermions that are strongly interacting through the experience of nuclear force. The most important baryons are the ones that form the baryon octet shown in figure 3.1.

The lightest and most familiar baryons are the proton and the neutron. The baryons interact with each other via the strong interaction, mediated by the exchange of *mesons*. Mesons are exchange particles made of a *quark* and an *antiquark*. Their spin adds up to integer numbers and therefore they are bosons and obey the Bose-Einstein statistics. The most important messengers between the baryons in a neutron star are the $\delta-$, $\omega-$ and the ρ mesons. Pions (π) and kaons ($K^+, K^0, \bar{K}^0, K^-$) can occur as condensates

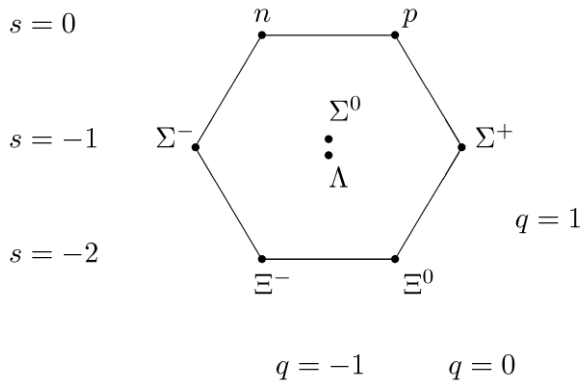

Figure 3.1: The most important baryons form the baryon octet, q refers to the electric charge and s to the strangeness quantum number. Credits: Wikipedia Bayron_octet.png .

in the inner core of neutron stars. Baryons and mesons are referred to as *hadrons*.
A possible matter constitution for a neutron star could be a mixture of neutrons, protons, electrons and, at higher densities, muons. At high matter densities the Fermi energies of the nucleons can become large enough that some of the nucleons transform via electroweak interaction into heavier baryons such as $\Lambda-$ and $\Sigma-$. For this reason in a neutron star there can be a large amount of species with lower Fermi momenta respect to neutrons. This leads to a pressure reduction and thus a softening of the equation of state. A softer equation of state lead to more compact stars as it takes higher densities to reach the pressure needed to balance gravity. This lead to neutron stars with small radius and relatively small maximum mass.

3.3 BL equation of state

A precise understanding of the equation of state of neutron stars is key to compute realistic simulation of compact binary mergers with at least one neutron star. Indeed, as it will be explained in chapter 6, in order to compute the love numbers for a neutron star it is needed to know the relation between the pressure and the energy density inside a neutron star. By definition, the equation of state is the relationships between matter pressure P, energy density ε, baryonic density n and temperature T together with information on the matter composition.
The derivation of an EOS suitable for the description of a neutron star requires a tremendous theoretical and computational effort, because of the huge density and temperature variations expected during the dynamical evolution of a merging neutron star. An EOS has to describe matter in a wide range of conditions, ranging from homogeneous matter down to a mixture of fully ionized atoms.
In the code written to compute the love number k_2 and explained in chapter 6, the EOS used is the Bombaci-Logoteta (BL) equation of state (ref. [3]) extended to finite temperature as explained in ref. [8].
In the models adopted in ref. [8] the neutron star core is modelled as a uniform charge-neutral fluid of neutrons, protons, electrons and muons. The EOS is calculated for arbitrary lepton fractions, densities, and temperatures. Even considering this simplified picture which does not take into account exotic degrees of freedom like hyperons or deconfined quarks, the determination of the EOS is still a a very challenging theoretical problem. In fact, the EOS has to be calculated under extreme condition of density, neutron-proton asymmetry and temperature, in a regime where the EOS is poorly constrained by nuclear data and experiments. The details of the derivation of the EOS are discussed in ref. [8]. The EOS can be used in tabulated form in numerical simulations, as it will be discussed in chapter 6. In the following

figures 3.2, 3.3 and 3.4 the quantities that enter in the EOS calculation (the pressure P, the energy density ε and the number density n) are shown as functions of the others.

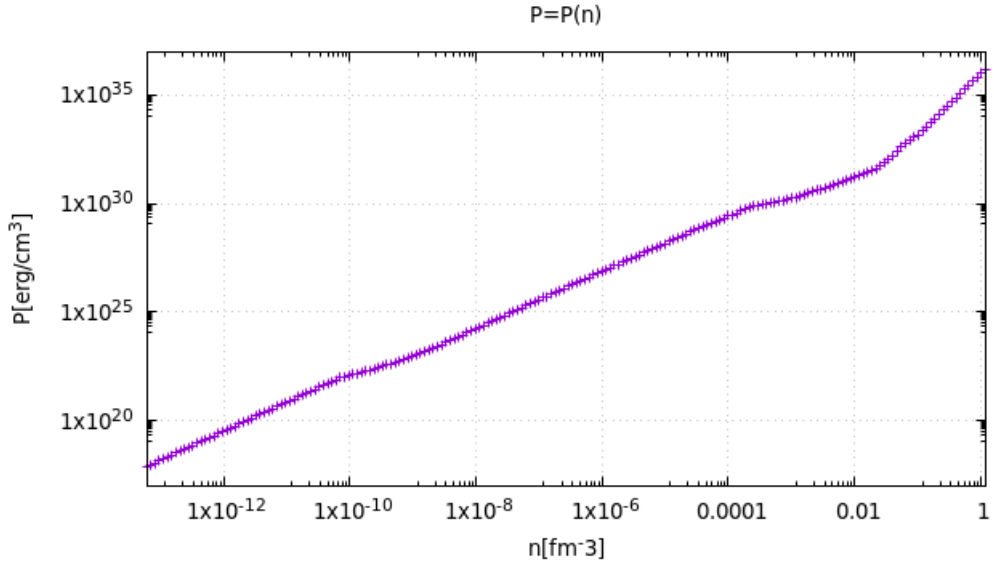

Figure 3.2: Plot in logarithmic scale of the pressure P in erg/cm^3 as function of the number density n in fm^{-3} for the BL equation of state. Courtesy of Domenico Logoteta (Pisa University).

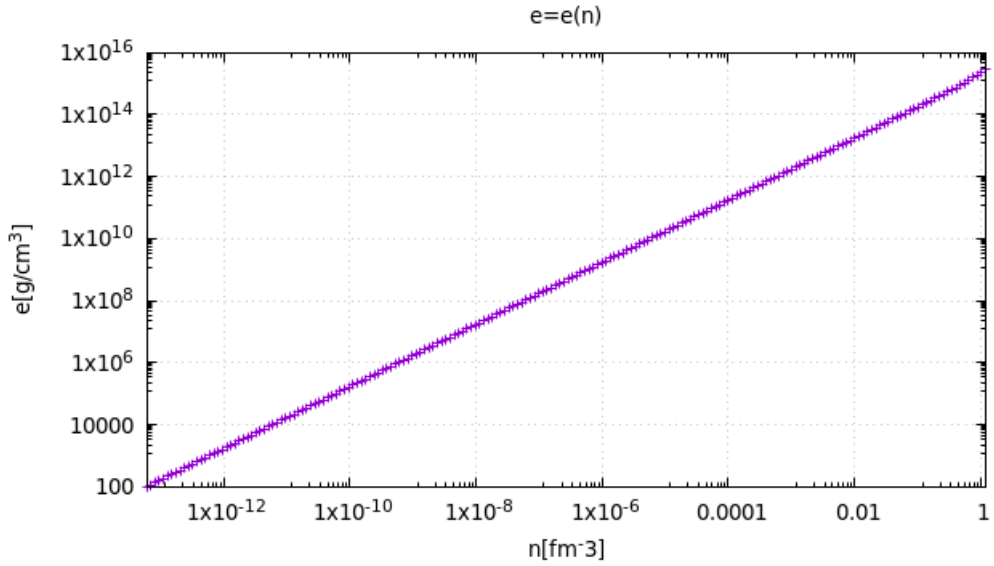

Figure 3.3: Plot in logarithmic scale of the energy density ε in g/cm^3 as function of the number density n in fm^{-3} for the BL equation of state. Courtesy of Domenico Logoteta (Pisa University).

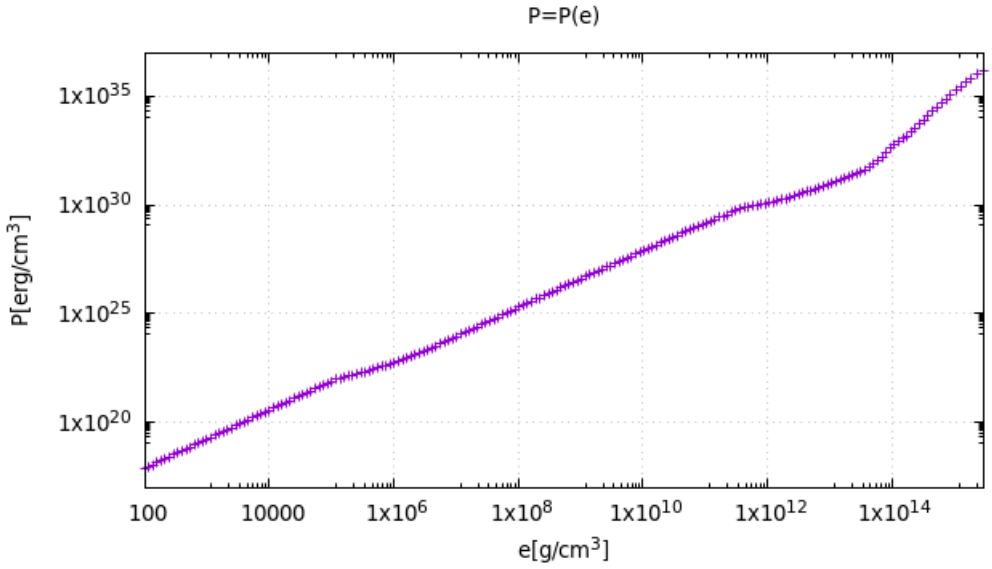

Figure 3.4: Plot in logarithmic scale of the pressure P in erg$/$cm^3 as function of the energy density ε in g$/$cm^3 for the BL equation of state. Courtesy of Domenico Logoteta (Pisa University).

Chapter 4

Compact binary systems

Half of the stars in the Universe are found in a system of two or more stars. These systems are called binary or multiple stellar systems. In particular, binary systems can contain one or two compact objects, such as neutron stars, white dwarfs and black holes. These systems are called compact binary systems. There are a lot of possible combinations for binary systems: every different compact object can be paired with another compact object or with another companion star. Every combination has his peculiarity. In this chapter we will follow ref. [15] in the study of general aspects of binary systems, starting from their dynamics. A discussion of the particular case of two neutron stars will follow.

4.1 Dynamics in a binary system

4.1.1 Orbital dynamics of two Newtonian point masses

If the distance between the two stars in a binary system is much larger than their stellar radius they can be approximated, from a dynamical point of view, as two point masses. The problem of motion of two point masses that interact gravitationally can be solved analytically reducing the problem to a one-body problem.
If we consider two point masses with masses m_1 and m_2 located at positions $\vec{r}_1$ and $\vec{r}_2$, their center of mass position is given by

$$\vec{R}_{CM} = \frac{m_1\vec{r}_1 + m_2\vec{r}_2}{m_1 + m_2} = \frac{m_1\vec{r}_1 + m_2\vec{r}_2}{M}, \tag{4.1}$$

where M is the total mass of the system. The force that body 2 exerts on body 1 is given by

$$\vec{F}_{21} = -G\frac{m_1 m_2}{|\vec{r}_1 - \vec{r}_2|^2}\hat{e}_r = m_1\ddot{\vec{r}}_1, \tag{4.2}$$

where $\hat{e}_r$ is the unit vector

$$\hat{e}_r = \frac{\vec{r}_1 - \vec{r}_2}{|\vec{r}_1 - \vec{r}_2|} = \frac{\vec{r}}{r}, \tag{4.3}$$

which points from body 2 to body 1. Note that $\vec{r}$ indicates the relative vector. The force exerted on body 2 by body 1 has the same magnitude but opposite sign for Newton's third law,

$$\vec{F}_{12} = -\vec{F}_{21} = G\frac{m_1 m_2}{|\vec{r}_1 - \vec{r}_2|^2}\hat{e}_r = m_2\ddot{\vec{r}}_2. \tag{4.4}$$

Therefore, the acceleration of the centre of mass vanishes as we expect from conservation of the total momentum,

$$\ddot{\vec{R}}_{CM} = \frac{m_1\ddot{\vec{r}}_1 + m_2\ddot{\vec{r}}_2}{M} = \frac{\vec{F}_{21} + \vec{F}_{12}}{M} = 0. \tag{4.5}$$

We can now express these equations using the coordinates $\vec{R}_{CM}$ and $\vec{r}$, as

$$\vec{r}_1 = \vec{R}_{CM} + \frac{m_2}{M}\vec{r}, \tag{4.6}$$

$$\vec{r}_2 = \vec{R}_{CM} - \frac{m_1}{M}\vec{r}. \tag{4.7}$$

Taking the second time derivative of 4.6 and 4.7 and multiplying the first one by m_1 and the second one by m_2 we obtain

$$m_1\ddot{\vec{r}}_1 = m_1\left(\ddot{\vec{R}}_{CM} + \frac{m_2}{M}\ddot{\vec{r}}\right) = \frac{m_1 m_2}{M}\ddot{\vec{r}}, \tag{4.8}$$

$$m_2\ddot{\vec{r}}_2 = m_2\left(\ddot{\vec{R}}_{CM} - \frac{m_1}{M}\ddot{\vec{r}}\right) = -\frac{m_1 m_2}{M}\ddot{\vec{r}}. \tag{4.9}$$

We can now introduce the *reduced mass*

$$\mu = \frac{m_1 m_2}{M}, \tag{4.10}$$

and confronting with equations 4.2 and 4.4 we can write

$$\mu\ddot{\vec{r}} = -\frac{G\mu M}{r^2}\hat{e}_r. \tag{4.11}$$

In this way the two equations of motion have been reduced to one equation for a fictitious body. Now we can solve the problem for this body with mass μ in a central field and than go back to the motion of the real bodies. In a central field the angular momentum is conserved and the motion is restricted to a plane. In this plane we can introduce the polar coordinates (r,ϕ) and use conservation of angular momentum and conservation of energy to derive the temporal evolution of these coordinates. The solutions are conic sections and Kepler's laws can be derived. In these coordinates

$$x(t) = r(t)\cos\phi(t), \tag{4.12}$$

$$y(t) = r(t)\sin\phi(t), \tag{4.13}$$

and the unit vectors $(\hat{e}_r,\hat{e}_\phi)$ are related to the unit vectors $(\hat{e}_x,\hat{e}_y)$ by

$$\hat{e}_r = \cos\phi\hat{e}_x + \sin\phi\hat{e}_y, \tag{4.14}$$

$$\hat{e}_\phi = -\sin\phi\hat{e}_x + \cos\phi\hat{e}_y. \tag{4.15}$$

The angular momentum becomes

$$\vec{L} = \vec{r}\times\mu\vec{v} = \mu r^2\dot{\phi}\hat{e}_z = L\hat{e}_z, \tag{4.16}$$

where $\hat{e}_z$ is the unit vector in the z-direction and L is the costant magnitude of the angular momentum. The *azimutal equation* is therefore

$$\frac{d\phi}{dt} = \frac{L}{\mu r^2}. \tag{4.17}$$

The square of the velocity is given by

$$|\vec{v}|^2 = \dot{x}(t)^2 + \dot{y}(t)^2 = \dot{r}^2 + r^2\dot{\phi}^2, \tag{4.18}$$

and therefore the conserved total energy is

$$E = \frac{\mu}{2}|\vec{v}|^2 - \frac{GM\mu}{r} = \frac{\mu}{2}\dot{r}^2 + \frac{\mu}{2}r^2\dot{\phi}^2 - \frac{GM\mu}{r} = \frac{\mu}{2}\dot{r}^2 + U_{\text{eff}}(r), \tag{4.19}$$

where $U_{\text{eff}}(r)$ is the effective potential

$$U_{\text{eff}}(r) = -\frac{GM\mu}{r} + \frac{L^2}{2\mu r^2} = -\frac{\alpha}{r} + \frac{\beta}{r^2}, \tag{4.20}$$

with $\alpha = G\mu M$ and $\beta = L^2/2\mu$. The second term is referred as *centrifugal potential*. Equation 4.19 solved for $\dot{r}$ gives the *radial equation*

$$\frac{dr}{dt} = \sqrt{\frac{2}{\mu}\left(E + \frac{\alpha}{r}\right) - \frac{L^2}{\mu^2 r^2}}. \tag{4.21}$$

Now we can introduce the parameters

$$p = \frac{L^2}{\mu\alpha}, \tag{4.22}$$

called the parameter of the orbit, and

$$e = \sqrt{1 + \frac{2EL^2}{\mu\alpha^2}}, \tag{4.23}$$

which is the eccentricity of the orbit. With these parameters, the solution of equation 4.21 can be written as

$$r = \frac{p}{1 + e\cos\phi}. \tag{4.24}$$

This is the equation of conic sections. The solutions can be:

- circles for $e = 0$;
- ellipses for $0 < e < 1$;
- parabola for $e = 1$;
- hyperbole for $e > 1$.

Kepler's first law, *the orbit of each planet is an ellipse with the Sun at one focus*, is included in the solution. It is important to note that bound orbits, like circles and ellipses, have a negative total energy as we expect and that circles are the orbits with minimum energy. Kepler's second law, *a line joining the planet and the star sweeps out equal areas dS during equal intervals of time dt*, is a direct consequence of conservation of angular momentum:

$$\frac{dS}{dt} = \frac{L}{2\mu} = const. \tag{4.25}$$

Kepler's third law, *the squares of the orbital periods are proportional to the cubes of the semimajor axes*, can be obtained by calculating the surface area S of an ellipse:

$$S = \int_0^P \frac{dS}{dt} dt = \frac{L}{2\mu} P, \tag{4.26}$$

where P is the orbital period. The surface of an ellipse is equal to $S = \pi ab$ where a and b are the semimajor and semiminor axes. Writing b as $b = a\sqrt{1-e^2}$ and using the definitions of a and e we obtain

$$P = 2\pi\sqrt{\frac{a^3}{GM}}, \tag{4.27}$$

which is exactly Kepler's third law. As said before, circular orbits are the ones with minimum energy. For this reason, a binary system that loses energy, for example for gravitational waves emission, tends to circularize.

4.1.2 Orbital evolution with gravitational waves emission

The theory of General Relativity predicts the emission of gravitational waves by a system with a time-varying quadrupole moment, like a binary system. The first direct observation of gravitational waves is dated September 2015 and was made by the LIGO collaboration. Nowadays, tens of detections have been reported. Gravitational waves are ripples in the curvature of space-time that travel at the speed of light and carry away energy and momentum (both linear and angular) from the source. As a result the orbit of the binary decays and the stars spiral toward each other. If we consider a binary system of total mass M, reduced mass μ, semimajor axis a and eccentricity e the total power emitted due to gravitational waves is

$$P_{GW} = \frac{32G^4\mu^2M^3}{5c^5a^5} f(e), \tag{4.28}$$

where

$$f(e) = \frac{1}{(1-e^2)^{7/2}} \left(1 + \frac{73}{24}e^2 + \frac{37}{96}e^4\right). \tag{4.29}$$

The angular momentum variation is instead given by

$$\frac{dL_{GW}}{dt} = -\frac{32G^{7/2}\mu^2M^{5/2}}{5c^5a^{7/2}} g(e), \tag{4.30}$$

where

$$g(e) = \frac{1}{(1-e^2)^2} \left(1 + \frac{7}{8}e^2\right). \tag{4.31}$$

In order to study the evolution of a binary system we need to know how its energy and angular momentum change with time. That is given by the conservation laws

$$\frac{dE_{BIN}}{dt} = -P_{GW}, \tag{4.32}$$

$$\frac{dL_{BIN}}{dt} = -\frac{dL_{GW}}{dt}. \tag{4.33}$$

To describe the orbit we are mainly interested in the evolution of the semimajor axis a and the eccentricity e. Knowing that

$$e = \sqrt{1 + \frac{2EL^2M}{G^2m_1^3m_2^3}}, \tag{4.34}$$

and

$$a = -\frac{Gm_1m_2}{2E}, \tag{4.35}$$

and using the relations

$$\frac{da}{dt} = \frac{da}{dE}\frac{dE}{dt}, \tag{4.36}$$

$$\frac{de}{dt} = \frac{\partial e}{\partial E}\frac{\partial E}{\partial t} + \frac{\partial e}{\partial L}\frac{\partial L}{\partial t}, \tag{4.37}$$

we can deduce the time evolution of the orbit's parameters

$$\frac{da}{dt} = -\frac{64}{5}\frac{G^3\mu M^2}{c^5a^3} f(e), \tag{4.38}$$

$$\frac{de}{dt} = -\frac{304}{15}\frac{G^3\mu M^2}{c^5a^4} \tilde{g}(e), \tag{4.39}$$

where $f(e)$ is the one given by equation 4.29 and

$$\tilde{g}(e) = \frac{e}{(1-e^2)^{5/2}}\left(1+\frac{121}{304}e^2\right). \tag{4.40}$$

We can note that $da/dt < 0$ and $de/dt < 0$ and therefore the orbit tends to circularize and scale down. Just before the final coalescence, typical neutron star binary orbits are close to circular.

4.2 Accretion mechanism

In the previous section we have discussed the dynamic evolution of a binary system assuming that the two stars were point masses and assuming that their mass is constant during the evolution. Sometimes this is not true. It is possible indeed for close binary systems to transfer mass from one star to the other and this can affect their orbit.

There are different ways in which this can happen. For example, in high-mass X-ray binaries (HMBXs) this can happen via strong wind or via the so-called Roche lobe overflow. The second one can happen when one of the star becomes comparable at some point to the size of the Roche lobe, which is the region around a star in a binary system within which orbiting material is gravitationally bound to that star. Now matter can flow over to the companion star via Lagrange point L_1 (the Lagrange point that lies in the line between the centers of the two stars) as shown in figure 4.1. The same can happen if the mutual separation shrinks to the point that the stellar radius is comparable to Roche lobe in size, as shown in figure 4.1 for a low-mass X-ray binary system (LMXB). Mass transfer does not only change

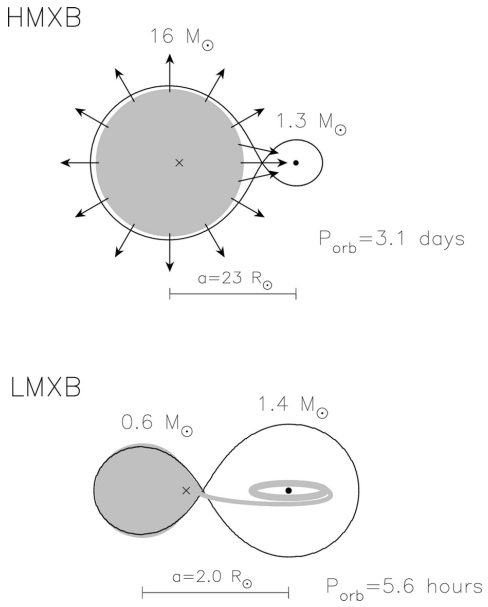

Figure 4.1: Examples of HMXB fed by a strong wind and LMXB in which case accretion occurs because of Roche lobe overflow. Credit: [17].

the masses but transfers also angular momentum and therefore it can change the orbital separation. For example, let's assume that mass is transferred from the lighter to the heavier component, we know that the center of mass cannot be accelerated by internal forces. Therefore, if the more massive component is becoming even more massive, the low-mass component has to move further out to keep the center of mass fixed. Instead if the mass is transferred from the heavier to the lighter component the orbital separation may decrease.

4.3 Double neutron star systems

4.3.1 Hulse-Taylor binary

In 1974 Russen Hulse and Joseph Taylor discovered a pulsar whose pulse frequency periodically shifted back and forth. The reason they come up with as explanation is that the pulsar had to be part of a binary system. Soon they observed the companion, which is a neutron star orbiting the pulsar in less than 8 hr. This system, called PSR 1913+16, was one of the first observational proof of the theory of General Relativity. In fact, the evolution of the system observed in more than 30 years is in perfect agreement with the predictions of the theory. In general, it is difficult to measure the semimajor axis of a binary system while it is much easier to measure the period P. For this reason, it is useful to consider the equation

$$\frac{1}{P}\frac{dP}{dt} = -\frac{96}{5}\frac{G^{5/3}\mu M^{2/3}}{c^5}\left(\frac{P}{2\pi}\right)^{-8/3} f(e), \tag{4.41}$$

which describes the relative variation of the period. In figure 4.2 it is shown the cumulative shift of periastron time of the system and the comparison with the general relativity predictions. The PSR 1913+16

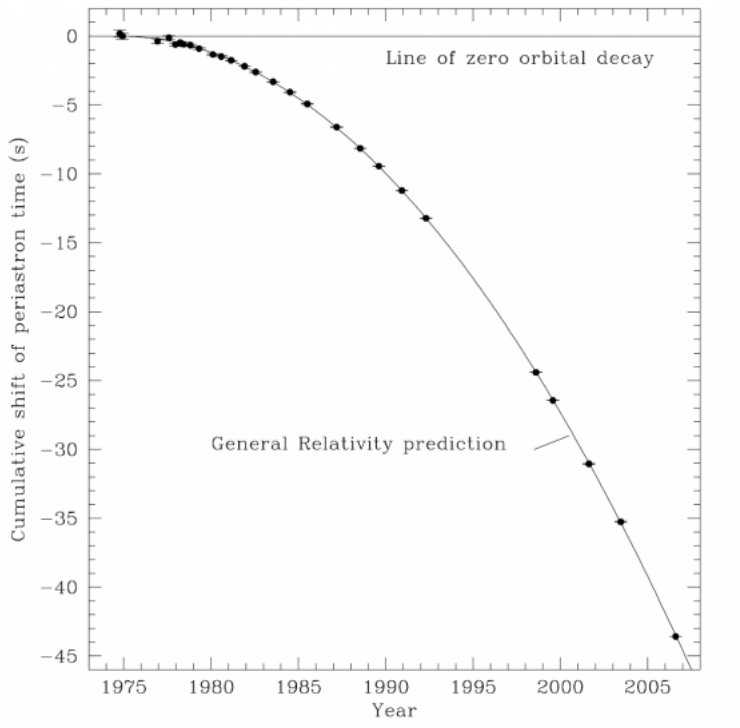

Figure 4.2: Cumulative shift period of the Hulse-Taylor binary (PSR 1913+16): comparison between experimental data and General Relativity predictions. Credits: [18].

has been a perfect gravitational laboratory. In fact the separation between the stars is large enough that tidal effects are completely negligible and the stars can be approximated as point masses. The orbit is tight enough and the eccentricity, $e = 0.62$ is large enough that the general relativistic effects can be measured. For instance, deviations from a $1/r$ potential lead to a slow motion of the periastron, an effect that has also been measured in the Solar System for the planet Mercury. The knowledge of the orbital parameters of PSR 1913+16 leads us to infer with accuracy the mass of both the neutron stars (about $1.4\,M_\odot$ each). The mass of the pulsar, $1.4414 M_\odot$, was the highest well-known neutron star mass for several time, but know we have detected more than one NS with mass equal or even superior to $2\,M_\odot$, like

the PSR J0740+6620, which has a mass of 2.08 $M_\odot$. The orbit of the binary system decays in excellent agreement with the gravitational waves predictions derived from General Relativity.

4.3.2 Formation channels

Double neutron stars systems (DNSs) are rare because the initial binary system has to survive two subsequent supernova explosions. Some fraction, however, survives as highly eccentric DNS. The are several paths that can lead to the formation of a DNS. If a star has an initial mass of less than $M_{SN} \approx 8M_\odot$ it will ends his life as a white dwarf. If the mass is more than M_{SN} but less than $M_{BH} \approx 25M_\odot$ the supernova explosion forms a neutron star. For masses heavier than M_{BH} a black hole forms. The formation of a DNS starts out from a close, massive binary system where both stars have masses between M_{SN} and M_{BH} and their separation is less than 1 AU. The heaviest star (the primary one) evolves faster and bloats up when evolving toward a giant phase and it can overflow its Roche lobe and transfer mass to its lower mass companion (the secondary). At the end of its life time the primary star forms a neutron star. If the system survives the core-collapse supernova explosion it consists of a neutron star and a main-sequence star. If the main sequence star transfer mass to the neutron star the system may be observable as a HMXB system. As the secondary star evolves further and bloats up, its evolved core and the neutron star revolve around each other inside the hydrogen envelope of the secondary. They lose orbital energy that is deposited in the envelope. When the envelope is ejected a system made up of a neutron star and the naked core of the second star (He-star) is left behind. The He-star will at some point produce a neutron star via supernovae explosion, and if the system survives this second explosion a DNS is left behind.

Chapter 5

Tidal deformation of neutron stars

In chapter 4 we have discussed the dynamics of a compact binary system, and in particular we have discussed the case of neutron binary systems. In these systems, the emission of gravitational waves causes a decrease of the energy and the angular momentum of the system and therefore the objects tend to become closer and closer, until they merge. In the final phase of the inspiral the tidal forces between the neutron stars tend to stretch the compact objects. The description of such events requires the general relativity theory, although a study of the Newtonian theory helps the comprehension of what happens. For this reason, in this chapter we will discuss the Newtonian formulation of tidal theory following ref. [4] and than we will briefly recall the equations that govern the tidal deformation from ref. [11] and [12]. In the last part of this chapter we will discuss the equations that lead to the calculation of the love number k_2 and how this coefficient describe the deformation of a neutron star following ref. [7] and [13].

5.1 Newtonian formulation

In Newtonian gravity the orbits of planets and stars are governed by Kepler's laws, derived in chapter 4. In that study the objects are treated as point masses, under the assumption that they are spherically symmetric. If we remove the assumption of spherical symmetry new forces appears, the tidal forces. Lets take the binary system Earth-Moon as example. One side of the moon is closer to the Earth than the other side, and therefore the Earth's gravitational force on a small test mass must be greater on the Moon's near side. For this reason the shape of the Moon is instantaneously elongated. For Newton's third law, the same situation must also apply to the near and far sides of Earth because of the gravitational influence of the Moon. This phenomenon happens in every binary system and it is called tidal deformation. The force on an object due to his non-zero size is known as a tidal force. The non spherical shape of the planet and the moon can influence their rotation rates by creating torques. In extreme cases it can happen that the tidal force is large enough that the smaller object could be disrupted.
On Earth tides are well known because of the presence of oceans. There are two high tides approximately every 25 h. Less well known are the tidal bulges of the solid Earth, which measure only about 10 cm in height. On the moon the bulges are much larger, as Earth is much more massive, resulting in nearly 20 m of deformation at its surface.

5.1.1 Physics of tides

Let's consider the force on a test mass m_1 located within the planet at a distance r from the Moon's center of mass,

$$F_{m_1} = G\frac{Mm_1}{r^2}, \tag{5.1}$$

where M is the mass of the Moon. Now we can take a second mass $m_2 = m_1 = m$, located at a distance dr from m_1 along the line connecting Earth to the Moon, as shown in figure 5.1. The difference between

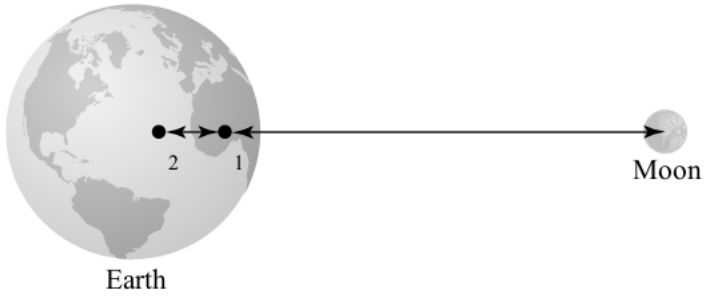

Figure 5.1: The tidal forces on Earth due to the Moon arise because of the different value of the gravitational force at different position within the Earth. Credits: [4].

the forces on the two test masses (the differential force) is

$$dF_m = \left(\frac{dF_m}{dr}\right) dr = -2G\frac{Mm}{r^3}dr. \tag{5.2}$$

It is important to note that the differential force decreases more rapidly then the force of gravity with distance and therefore the further away the masses are to the moon the less pronounced the effect is. To understand the shape of the tidal bulges on Earth we have to analyze the differences in the gravitational force vectors acting at the center of the planet and at some point on its surface. Let's consider only the forces on the x-y plane, taking the x-axis as the line between the centers of Earth and Moon and the y-axis as shown in figure 5.2. Neglecting rotation, the effects are symmetric about the x-axis. The components

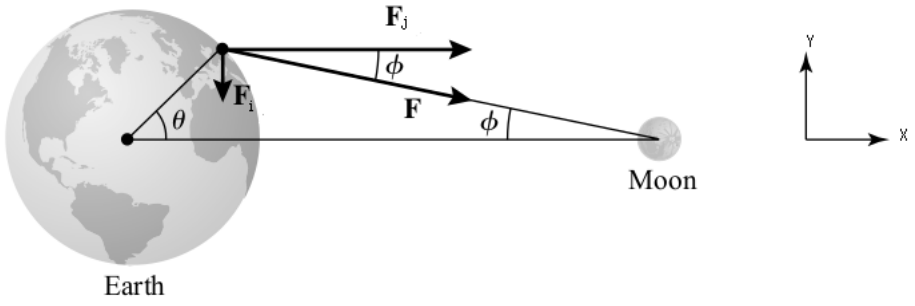

Figure 5.2: The geometry of tidal forces acting on Earth due to the Moon. Credits: [4].

of the force on a mass m located at the center of Earth are

$$F_{C,x} = G\frac{Mm}{r^2}, \tag{5.3}$$

$$F_{C,y} = 0, \tag{5.4}$$

while at a point P on the surface the components are

$$F_{P,x} = \frac{GMm}{s^2}\cos\phi, \tag{5.5}$$

$$F_{P,y} = -\frac{GMm}{s^2}\sin\phi, \tag{5.6}$$

where s is the distance between the center of the Moon and the point P and ϕ is the angle shown in figure 5.2. The differential force between the center of Earth and a point on his surface is

$$\Delta\mathbf{F} = \mathbf{F}_P - \mathbf{F}_C = GMm\left(\frac{\cos\phi}{s^2} - \frac{1}{r^2}\right)\hat{\mathbf{i}} - \frac{GMm}{s^2}\sin\phi\hat{\mathbf{j}}, \tag{5.7}$$

where $\hat{\mathbf{i}}$ and $\hat{\mathbf{j}}$ are the unit vectors along the x-axis and along the y-axis. Now we can write s in terms of r, R and θ, where r is the distance between the centers of Earth and Moon, R is the radius of Earth and θ is the angle shown in figure 5.2:

$$s^2 = (r - R\cos\theta)^2 + (R\sin\theta)^2 \simeq r^2\left(1 - \frac{2R}{r}\cos\theta\right), \tag{5.8}$$

where the terms of order $R^2/r^2 \ll 1$ or higher have been neglected. Substituting this expression in equation 5.7 and recalling that for $x \ll 1$, $(1+x)^{-1} \simeq 1-x$ we obtain that

$$\Delta\mathbf{F} \simeq \frac{GMm}{r^2}\left[\cos\phi\left(1 + \frac{2R}{r}\cos\phi\right) - 1\right]\hat{\mathbf{i}} - \frac{GMm}{r^2}\left[1 + \frac{2R}{r}\cos\theta\right]\sin\phi\hat{\mathbf{j}}. \tag{5.9}$$

Using the first order relations $\cos\phi \simeq 1$ and $\sin\phi \simeq (R\sin\theta)/r$ we have

$$\Delta\mathbf{F} \simeq \frac{GMmR}{r^3}\left(2\cos\theta\hat{\mathbf{i}} - \sin\theta\hat{\mathbf{i}}\right). \tag{5.10}$$

We note that there is an extra factor 2 in the x-component when compared with the y-component. The situation is shown in figure 5.3. The force vectors act to compress Earth in the y-direction and elongate it along the x-direction, producing tidal bulges.

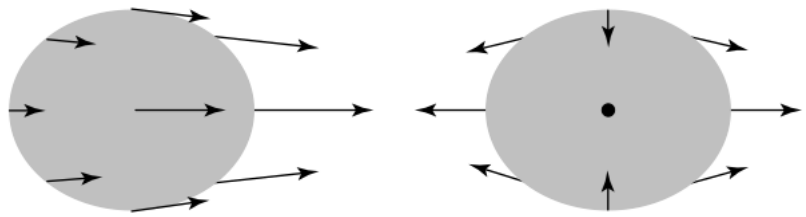

Figure 5.3: (a) The gravitational force of the Moon on Earth. (b) The differential gravitational force on Earth, relative to its center. Credits: [4].

5.2 General relativity tidal theory

In general relativity, the inspiral phase of neutron stars binaries can be studied with a post Newtonian expansion, eventually improved with the Effective One Body (EOB) technique. In this phase, the NS is deformed because of tidal effects that depend on the equation of state of the NS. In the next section we will discuss the theory in the Newtonian approximation, while in the following one we will have a more qualitative discussion of the theory in general relativity.

5.2.1 Newtonian approximation

In Newtonian gravity the external gravitational potential U_{ext} generates a quadrupolar tidal field

$$\mathscr{E}_{ij} = -\partial_i\partial_j U_{\text{ext}}. \tag{5.11}$$

Note that outside the body that generates it, U_{ext} obey to the equation $\nabla^2 U_{\text{ext}} = 0$ and therefore $\mathscr{E}_{ij}$ is both symmetric and traceless. That tidal field generates a perturbation δp in the equilibrium position of the NS. The gravitational potential generated by a deformed NS in the Newtonian approximation is, as shown in ref. [11],

$$U(t,\mathbf{x}) = G\int d^3x' \frac{\bar{\rho}(r') + \delta\rho(t,\mathbf{x}')}{|\mathbf{x}-\mathbf{x}'|}, \tag{5.12}$$

where $\bar{\rho}$ is the equilibrium configuration and $\delta\rho$ is the perturbation induced by the external gravitational field. Outside the neutron star we can perform the multipole expansion

$$\frac{1}{|\mathbf{x}-\mathbf{x}'|} = \frac{1}{r} + \frac{x_i}{r^3}x_i' + \frac{3\hat{x}_i\hat{x}_j - \delta_{ij}}{2r^3}x_i'x_j' + ..., \tag{5.13}$$

where $r = |\mathbf{x}|$, $\hat{x}_i = x_i/r$ and the expansion is valid for $r' < r$. Using this expansion in equation 5.12, the first term gives the unperturbed monopole contribution Gm/r (m is the NS mass), the second term is a dipole contribution proportional to $\int d^3x'\rho(t,\mathbf{x}')x_i'$ and vanishes because of the definition of the center of mass. The following term is the second moment of the mass density,

$$M_{ij}(t) = \int d^3x'\rho(t,\mathbf{x}')x_i'x_j'. \tag{5.14}$$

In U, M_{ij} is multiplied by the traceless tensor $3\hat{x}_i\hat{x}_j - \delta_{ij}$ and therefore we can replace M_{ij} with the traceless quadrupole moment

$$Q_{ij}(t) = \int d^3x'\rho(t,\mathbf{x}')\left(x_i'x_j' - \frac{1}{3}r'^2\delta_{ij}\right). \tag{5.15}$$

Note that, because $\bar{\rho}$ is spherical symmetric, only $\delta\rho(t,\mathbf{x}')$ contributes to Q_{ij}. Outside the NS we can add the potential generated by the deformed NS to the external potential U_{ext} written as an expansion around the center of mass of the NS:

$$U_{ext} = -\frac{1}{2}\mathscr{E}_{ij}x_ix_j + \mathscr{O}(x^3). \tag{5.16}$$

Using $Q_{ij}\delta_{ij} = 0$ we get

$$U(t,\mathbf{x}) = \frac{Gm}{r} + \frac{3G}{2r^3}\hat{x}_i\hat{x}_jQ_{ij}(t) + \mathscr{O}\left(\frac{1}{r^4}\right) - \frac{1}{2}\mathscr{E}_{ij}(t)x_ix_j + \mathscr{O}(x^3). \tag{5.17}$$

If the external perturbation $\mathscr{E}_{ij}$ can be considered as static and therefore also the induced quadrupole Q_{ij} is time independent, then $U = U(\mathbf{x})$ is only function of $\mathbf{x}$. In the case of static or quasi-static perturbation the induced quadrupole can be written to the linear order as

$$Q_{ij}(t) = -\lambda\mathscr{E}_{ij}(t), \tag{5.18}$$

for some constant λ.
The $l = 2$ tidal Love number k_2 is defined as

$$k_2 = \frac{3}{2}\frac{G\lambda}{R^5}, \tag{5.19}$$

where R is the neutron star radius, and it is dimensionless. With this definition, equation 5.18 becomes

$$Q_{ij} = -\frac{2}{3G}k_2R^5\mathscr{E}_{ij}. \tag{5.20}$$

The corresponding compoment g_{00} of the metric in the Newtonian approximation is given by $g_{00} = -1 + 2U/c^2$, and therefore

$$g_{00} = -1 + \frac{2Gm}{c^2 r} - \frac{1}{c^2}\mathscr{E}_{ij}(t)x_i x_j \left[1 + 2k_2 \left(\frac{R}{r}\right)^5\right] + \mathscr{O}\left(\frac{1}{r^4}\right) + \mathscr{O}(x^3). \tag{5.21}$$

The procedure followed to obtain the Love number k_2 can be generalized to obtain the Love number k_l, considering higher multipole contribution to the external field. For this aim, we need to introduce the tensor

$$\mathscr{E}_{i_1,i_2,\ldots i_l} = -\frac{1}{(l-2)!}\partial_{i_1}\ldots\partial_{i_l}U_{\text{ext}}, \tag{5.22}$$

which is symmetric and traceless in all its indices. We can define the Love number k_l for each Newtonian multipole using

$$g_{00} = -1 + \frac{2Gm}{c^2 r} - \frac{1}{c^2}\sum_{l=2}^{\infty}\frac{2}{l(l-1)}\mathscr{E}_{i_1\ldots\ldots 1_l}x^i\ldots x^{i^l}\left[1 + 2k_l\left(\frac{R}{r}\right)^{2l+1}\right]. \tag{5.23}$$

This result can be written in a more compact way by introducing the multi-index notation

$$\mathscr{E}_L = -\frac{1}{(l-2)!}\partial_L U_{ext}, \tag{5.24}$$

and g_{00} becomes

$$g_{00} = -1 + \frac{2Gm}{c^2 r} - \frac{1}{c^2}\sum_{l=2}^{\infty}\frac{2}{l(l-1)}\mathscr{E}_L x^L\left[1 + 2k_l\left(\frac{R}{r}\right)^{2l+1}\right]. \tag{5.25}$$

5.2.2 General relativity theory

The Newtonian approximation developed in the previous section has only limited accuracy for NS. The appropriate framework for the computation of tidal effects is the general-relativistic perturbation theory. A discussion of the methods of solution can be found in ref. [12]. The main steps are to find the solution of the perturbed equations outside the NS (the exterior problem) and inside the NS (the interior problem). The metric perturbations in the exterior problem separate into polar and axial modes for each multipole. The coefficient of these modes define two classes of Love number, corresponding to polar and axial modes and called *electric-type* and *magnetic-type* Love numbers, indicated with $k_l^{(e)}$ and $k_l^{(m)}$ respectively. In the Newtonian limit, the magnetic-type multipoles disappear and remains only a family of Newtonian multipoles, parametrized by the Newtonian Love numbers introduced in equation 5.25. In general relativity, anyway, there are two sets of electric-type and magnetic-type Love numbers.
Instead of equation 5.11 in general relativity the tidal field is described by

$$\mathscr{E}_{ij} = c^2 R_{0i0j}, \tag{5.26}$$

where $R_{\mu\nu\rho\sigma}$ is the Riemann tensor.
In order to compute the Love numbers one has to solve the interior problem and match the interior and exterior solutions on the boundary of the NS. Typical values of the Love number k_2 for a realistic EOS is $k_2 \simeq 0.05 - 0.15$.
With the induced quadrupole moment one can compute its effect in the dynamics of the binary system. This gives a correction of the order $\mathscr{O}(v/c)^{10}$, which is a 5 post Newtonian correction.
It is useful to introduce, for each neutron star of a binary system, the quantity

$$\Lambda_i = \frac{2}{3}k_2\left(\frac{R_i}{Gm_i/c^2}\right)^5, \tag{5.27}$$

where R_i and m_i are the radius and the mass of the i-th NS. This quantity is the tidal deformability of a NS. Λ_i is dimensionless and it is proportional to the fifth power of radius R_i. Typical values of Λ_i are of order $10^2 - 10^3$. Given Λ_1 and Λ_2 for two NSs in a binary system we can define

$$\tilde{\Lambda} = \frac{16}{13} \frac{(m_1 + 12m_2)m_1^4\Lambda_1 + (m_2 + 12m_1)m_2^4\Lambda_2}{(m_1 + m_2)^5}, \tag{5.28}$$

which is the combined dimensionless tidal deformability of a binary neutron star system, a parameter that can be inferred from gravitational waves detection experiments and confronted with the theory. Typically the tidal deformability for a NSs merger is $\tilde{\Lambda} \leq 800$, assuming low NS spins.

5.3 Love number k_2 equations

In this section we will introduce the equations to calculate the Love number k_2. More details on their derivation can be found in ref. [7] and [13]. As explained in the previous section, the tidal deformability parameter λ is defined as

$$Q_{ij} = -\lambda \mathscr{E}_{ij}, \tag{5.29}$$

where Q_{ij} is the induced quadrupole moment of a star in a binary due to the static external field $\mathscr{E}_{ij}$ of the companion star. The parameter λ is related to the dimensionless Love number k_2 as

$$\lambda = \frac{2}{3} \frac{k_2 R^5}{G}, \tag{5.30}$$

where R is the radius of the NS. We expect, for a neutron star, a value of k_2 between 0.05 and 0.15. This quantity is given by

$$k_2 = \frac{8C^5}{5}(1-2C)^2 [2 + 2C(y_R - 1) - y_R] \Big\{ 2C[6 - 3y_R + 3C(5y_R - 8)] + 4C^3[12 - 11y_R + C(3y_R - 2) + 2C^2(1 + y_R)] + 3(1-2C)^2[2 - y_R + 2C(y_R - 1)] \times \ln(1-2C) \Big\}^{-1}, \tag{5.31}$$

where

$$C = \frac{GM}{c^2 R}, \tag{5.32}$$

is the compactness parameter of the star. In equation 5.31 $y_R = y(R)$ is the value at distance R of the radial function $y(r)$, solution of the differential equation

$$r\frac{dy(r)}{dr} + y(r)^2 + y(r)F(r) + r^2 Q(r) = 0, \tag{5.33}$$

with

$$F(r) = \frac{r - \frac{4\pi G\, r^3}{c^4}[\varepsilon(r) - P(r)]}{r - \frac{2m(r)G}{c^2}}, \tag{5.34}$$

$$Q(r) = \frac{\frac{4\pi\, G\, r}{c^4}\left[5\varepsilon(r) + 9P(r) + \frac{\varepsilon(r) + P(r)}{\partial P(r)/\partial \varepsilon(r)}\right] - \frac{6}{4\pi r^2}}{r - \frac{2Gm(r)}{c^2}} - 4\left[\frac{\frac{Gm(r)}{c^2} + 4\pi\frac{Gr^3 P(r)}{c^4}}{r^2\left[1 - \frac{2Gm(r)}{c^2 r}\right]}\right]^2. \tag{5.35}$$

To solve equation 5.33 one has to use the initial condition $y(0) = 2$.

Chapter 6

Computation of the Love number k_2

In this chapter we will explain the method used to compute the Love number k_2 of a neutron star with the BL equation of state introduced in chapter 3 . The process consists in the numerical integration of the equations reported in section 5.3 together with the TOV equations introduced in section 2.6.2, as it will be explained in section 6.1. The numerical integrator used is Runge-Kutta 4th order for multiple variables. The code, written in the C language, can be found in appendix A.1.

6.1 Dimensionless units and equations to integrate

In order to integrate the equations it is important to write them in dimensionless form to avoid numerical errors. We can start from the TOV equations 2.22 and 2.23 where we need to choose the scaling relations for mass, radius, pressure and energy density. We can write each quantity as

$$m = \bar{m}\, m_0, \tag{6.1}$$

$$r = \bar{r}\, r_0, \tag{6.2}$$

$$P = \bar{P}\, P_0, \tag{6.3}$$

$$\varepsilon = \bar{\varepsilon}\, \varepsilon_0, \tag{6.4}$$

where the quantities on the left are the dimensional ones, the barred quantities on the right are the dimensionless ones (the ones used in the code for integration) and the coefficients with the subscript are the scaling relations. If we substitute these expressions in equations 2.22 and 2.23 and we choose the scaling relations such as they satisfy

$$1 = \frac{r_0^3 \varepsilon_0}{m_0 c^2}, \tag{6.5}$$

$$1 = G\frac{\varepsilon_0 m_0}{c^2 r_0 P_0}, \tag{6.6}$$

$$1 = \frac{P_0}{\varepsilon_0}, \tag{6.7}$$

the dimensionless TOV equations become

$$\frac{d\bar{m}}{d\bar{r}} = 4\pi \bar{r}^2 \bar{\varepsilon}, \tag{6.8}$$

$$\frac{d\bar{P}}{d\bar{r}} = -\frac{(\bar{P}+\bar{\varepsilon})(\bar{m}+4\pi\bar{r}^3\bar{P})}{\bar{r}^2 - 2\bar{m}\bar{r}}. \tag{6.9}$$

About the request 6.7, we note that energy density and pressure have the same dimensions, therefore it is natural to use the same scaling coefficient for them.
We have chosen

$$r_0 = 10000\,\mathrm{m} = 10\mathrm{km}, \tag{6.10}$$

because it is of the magnitude order of the radius of a typical neutron star. The other scaling coefficients are the given by 6.5, 6.6 and 6.7:

$$m_0 = \frac{c^2 r_0}{G} \simeq 1.35 \cdot 10^{31}\mathrm{kg} \simeq 6.77\mathrm{M}_\odot, \tag{6.11}$$

$$P_0 = \varepsilon_0 = \frac{c^4}{r_0^2 G} \simeq 1.21 \cdot 10^{36}\mathrm{J\ m^{-3}}, \tag{6.12}$$

where $c = 299792458\mathrm{m/s}$ and $G = 6.6725 \cdot 10^{-11}\mathrm{m^3\,kg^{-1}\,s^{-2}}$. For the sake of clarity, we report in table 6.1 the scaling relations used. For the equations of the Love number k_2 we can follow the same procedure

Quantities	Symbols	Units	Value
Radius	r_0	m	$1.0 \cdot 10^4$
Mass	m_0	kg	$1.34695418 \cdot 10^{31}$
energy density	ε_0	$\mathrm{Jm^{-3}}$	$1.21058205 \cdot 10^{36}$
Pressure	P_0	$\mathrm{Jm^{-3}}$	$1.21058205 \cdot 10^{36}$

Table 6.1: Scaling relations chosen to write the equations in dimensionless form.

with the same scaling relations 6.5, 6.6 and 6.7 to write them in dimensionless form. Equation 5.31 remains the same, as k_2, the compactness C and the quantity y_R are already dimensionless for definition. Equations 5.33, 5.34 and 5.35 become instead:

$$\bar{r}\frac{dy(\bar{r})}{d\bar{r}} + y(\bar{r})^2 + y(\bar{r})F(\bar{r}) + \bar{r}^2 Q(\bar{r}) = 0, \tag{6.13}$$

$$F(\bar{r}) = \frac{\bar{r} - 4\pi\bar{r}^3[\bar{\varepsilon}(\bar{r}) - \bar{P}(\bar{r})]}{\bar{r} - 2\bar{m}(\bar{r})}, \tag{6.14}$$

$$Q(\bar{r}) = \frac{4\pi\bar{r}[5\bar{\varepsilon}(\bar{r}) + 9\bar{P}(\bar{r}) + \dfrac{\bar{\varepsilon}(\bar{r}) + \bar{P}(\bar{r})}{\partial\bar{P}(\bar{r})/\partial\bar{\varepsilon}(\bar{r})} - \dfrac{6}{4\pi\bar{r}^2}]}{\bar{r} - 2\bar{m}(\bar{r})} - 4\left[\frac{\bar{m}(\bar{r}) + 4\pi\bar{r}^3\bar{P}(\bar{r})}{\bar{r}^2 aa\,[1 - 2\bar{m}(\bar{r})/\bar{r}]}\right]^2. \tag{6.15}$$

In the code, $\bar{m}(\bar{r})$ is the mass enclosed within the radius $\bar{r}$, $\bar{\varepsilon}(\bar{r})$ is the energy density at distance $\bar{r}$ from the center and $\bar{P}(\bar{r})$ is the pressure. These quantities, expressed as dimensionless, can be obtained integrating the TOV equations 6.8 and 6.9 considering the information of the EOS that relates the pressure and the energy density, as explained in section 6.3. Together with TOV equations we can integrate equations 5.31, 6.13, 6.14 and 6.15 in order to obtain the Love number k_2. The initial conditions are $y(0) = 2$, $P(0) = P_c$ and $m(0) = 0$, where P_c is the central pressure of the neutron star. The numerical integration terminates when the pressure vanishes, which from a computational point of view means that the integration process ends when the pressure is smaller than an arbitrary number. Varying the central pressure P_c we obtain a sample of mass M, radius R and Love number k_2 for neutron stars with the BL EOS.

6.2 Runge-Kutta IV

Runge-Kutta 4th order method is a numerical technique to solve first order ordinary differential equations. In our case, the problem to solve is of the type

$$\begin{cases} \frac{dP}{dr} = f(r,P,m,y) \\ \frac{dm}{dr} = g(r,P,m,y) \\ \frac{dy}{dr} = u(r,P,m,y) \\ P(0) = P_c \\ m(0) = 0 \\ y(0) = 2 \end{cases} . \tag{6.16}$$

The techniques consists in adjourning the variables $P(r)$, $m(r)$ and $y(r)$ at every step of integration as:

$$\begin{cases} P_{n+1} = P_n + (k_1 + 2\cdot k_2 + 2\cdot k_3 + k_4)/6 \\ m_{n+1} = m_n + (l_1 + 2\cdot l_2 + 2\cdot l_3 + l_4)/6 \\ y_{n+1} = y_n + (d_1 + 2\cdot d_2 + 2\cdot d_3 + d_4)/6 \end{cases} , \tag{6.17}$$

where

$$\begin{cases} k_1 = h\cdot f(r,P_n,m_n,y_n) \\ l_1 = h\cdot g(r,P_n,m_n,y_n) \\ d_1 = h\cdot u(r,P_n,m_n,y_n) \end{cases} , \tag{6.18}$$

$$\begin{cases} k_2 = h\cdot f(r+\frac{h}{2},P_n+\frac{k_1}{2},m_n+\frac{l_1}{2},y_n+\frac{d_1}{2}) \\ l_2 = h\cdot g(r+\frac{h}{2},P_n+\frac{k_1}{2},m_n+\frac{l_1}{2},y_n+\frac{d_1}{2}) \\ d_2 = h\cdot u(r+\frac{h}{2},P_n+\frac{k_1}{2},m_n+\frac{l_1}{2},y_n+\frac{d_1}{2}) \end{cases} , \tag{6.19}$$

$$\begin{cases} k_3 = h\cdot f(r+\frac{h}{2},P_n+\frac{k_2}{2},m_n+\frac{l_2}{2},y_n+\frac{d_2}{2}) \\ l_3 = h\cdot g(r+\frac{h}{2},P_n+\frac{k_2}{2},m_n+\frac{l_2}{2},y_n+\frac{d_2}{2}) \\ d_3 = h\cdot u(r+\frac{h}{2},P_n+\frac{k_2}{2},m_n+\frac{l_2}{2},y_n+\frac{d_2}{2}) \end{cases} , \tag{6.20}$$

$$\begin{cases} k_4 = h\cdot f(r+h,P_n+k_3,m_n+l_3,y_n+d_3) \\ l_4 = h\cdot g(r+h,P_n+k_3,m_n+l_3,y_n+d_3) \\ d_4 = h\cdot u(r+h,P_n+k_3,m_n+l_3,y_n+d_3) \end{cases} , \tag{6.21}$$

and h is the pass of integration. Integrating with this methods brings an error of the order $\mathcal{O}(h^4)$.

6.3 Interpolation of EOS

In order to integrate the TOV equations together with equation 6.13 we need to extract information from the equation of state of the neutron star about energy density and pressure. In particular, we need to express the energy density as function of the pressure $\bar{\varepsilon} = \bar{\varepsilon}(\bar{P})$. In this way in equation 6.9 we can express all the terms as function of $\bar{P}$ and we can do the same in the expression 6.14. In equation 6.15 we need, other than $\bar{\varepsilon} = \bar{\varepsilon}(\bar{P})$, also $d\bar{P}/d\bar{\varepsilon} = d\bar{P}/d\bar{\varepsilon}(\bar{P})$. Having this information is the same as having $d\bar{\varepsilon}/d\bar{P} = d\bar{\varepsilon}/d\bar{P}(\bar{P})$ because of the inverse function rule. In the code written and reported in appendix A.1 the problem has been solved by using the linear interpolation technique. This technique works well enough because the tabulated EOS is sufficiently dense.
The code reads in input the BL sequence, described in chapter 3, and saves two vectors that contain the

dimensionless pressure $\bar{P}$ and the corresponding dimensionless energy density $\bar{\varepsilon}$. We indicate with $\bar{P}[n]$ and $\bar{\varepsilon}[n]$ the nth-element of the vectors. We want to write two functions that given a value of pressure return the corresponding value of energy density and the corresponding value of $d\bar{\varepsilon}/d\bar{P}$. Let's focus on the first one. It is useful to work with the logarithm of the vectors $\bar{P}$ and $\bar{\varepsilon}$ because we have to deal with different orders of magnitude. The first thing to do, given a value of pressure $\bar{P}^*$, is to find the index n such as $\bar{P}^* > \bar{P}[n]$ and $\bar{P}^* < \bar{P}[n+1]$. With the index n known, we can implement the formula

$$\bar{\varepsilon}^*(\bar{P}^*) = \bar{\varepsilon}[n](1-\alpha) + \bar{\varepsilon}[n+1]\alpha, \tag{6.22}$$

where

$$\alpha = \frac{\bar{P}^* - \bar{P}[n]}{\bar{P}[n+1] - \bar{P}[n]}. \tag{6.23}$$

In the code all the steps are made by using the base 10 logarithm of $\bar{P}$ and $\bar{\varepsilon}$ and the output of the procedure is then raised to the tenth power to restore the right value as output of the function.
For the function $d\bar{\varepsilon}/d\bar{P}$ we follow the same procedure but at the end the value of the derivative is given by

$$\frac{d\bar{\varepsilon}}{d\bar{P}}(\bar{P}^*) = \frac{\bar{\varepsilon}[n+1] - \bar{\varepsilon}[n]}{\bar{P}[n+1] - \bar{P}[n]}. \tag{6.24}$$

Note that in this case we cannot use the logarithm of the arrays, as before, because the incremental ratio of the logarithm raised to the tenth power is different from the incremental ratio of the quantities.

6.4 Results

In this section we will present and discuss the results of the code. The sequence obtained as output is reported in appendix A.2 and it consists in a sequence of possible value of the physical quantities mass, radius, compactness and Love number k_2 that correspond to a given central pressure, for a neutron star with BL equation of state. Note that the dimensionless value obtained from the integration process have been multiplied by the respective scaling coefficient (written in table 6.1) to obtain the physical value.

6.4.1 Mass-radius diagram

The resulting mass-radius diagram is the one shown in figure 6.1. As we expect for a compact object the radius decrease with the increasing of the mass (the inverse of what happens for ordinary stars) and the typical radius for a neutron star is between 12 and 13 km. The mass cannot reach arbitrary values but it has a maximum of about $2.102\,\mathrm{M}_\odot$. In figures 6.2 and 6.3 we plot the trend of compactness respect to radius and mass.

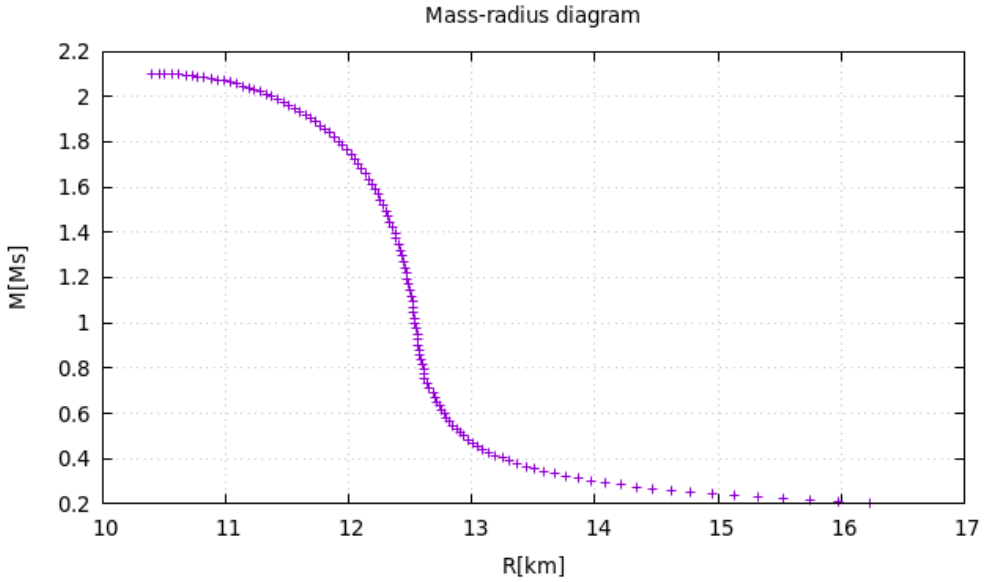

Figure 6.1: Diagram of mass in solar masses $M_{\odot}$ as function of the radius in km for neutron stars with BL equation of state.

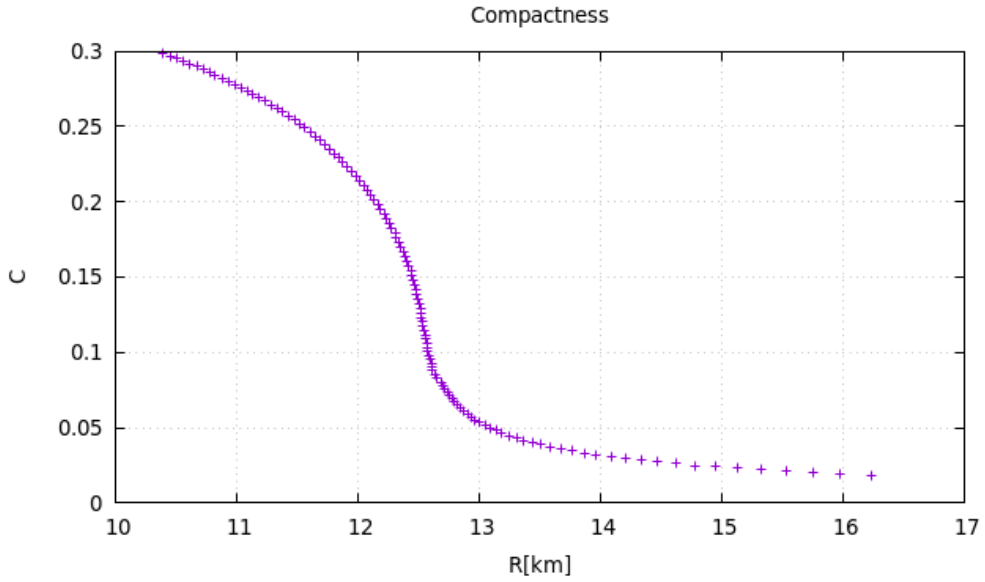

Figure 6.2: Diagram of the compactness as function of the radius in km for neutron stars with BL equation of state.

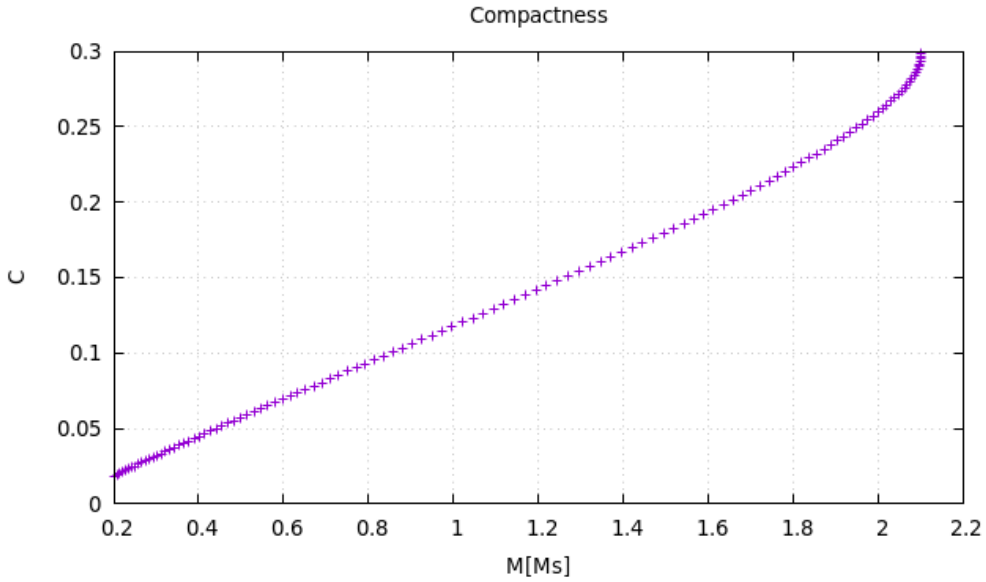

Figure 6.3: Diagram of the compactness as function of the mass in solar masses $M_\odot$ for neutron stars with BL equation of state.

6.4.2 Love number k_2

As anticipated in chapter 5 the typical value of the Love number k_2 for a neutron star is between 0.05 and 0.15 and our result is compatible with this range of value. The trends of k_2 as function of the radius and the mass are shown in figure 6.4 and 6.5.

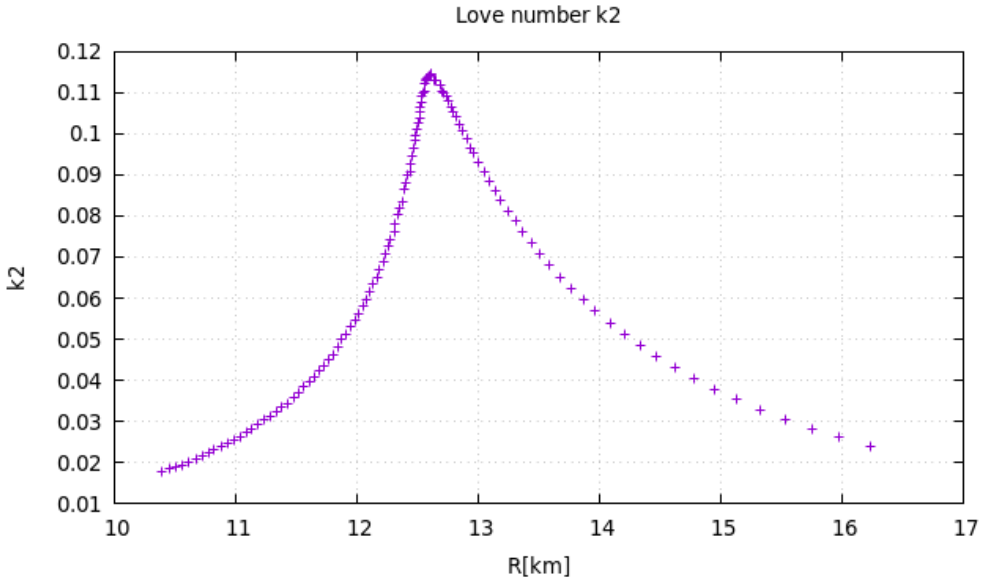

Figure 6.4: Diagram of the Love number k_2 as function of the radius in km for neutron stars with BL equation of state.

In figure 6.4 we note that the trend has a cusp for a radius that is between 12.5 and 13 km and that is a typical trend for low masses neutron stars (mass less than $1\,M_\odot$) that are very rare in nature.

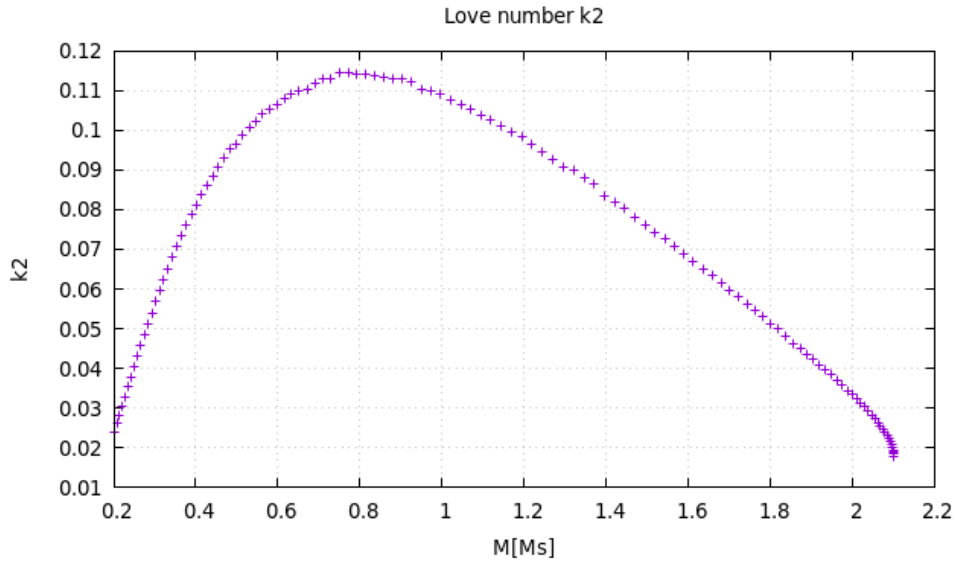

Figure 6.5: Diagram of the Love number k_2 as function of the mass in solar masses $M_\odot$ for neutron stars with BL equation of state.

6.5 Comparison with others results

Our results can be confronted with the results obtained using a public code available on Bitbucket's repositories. Such Matlab code solves the TOV equations in general relativity together with even/odd stationary perturbations for barotropic fluids and for arbitrary multipolar index. The reference papers for such code are [6] and [2].
In figures 6.6, 6.7, 6.8 and 6.9, 6.10 are plotted our results (in purple) and the results obtained with the public Matlab code (in green). As shown, our results seem to be compatible with the reference ones.

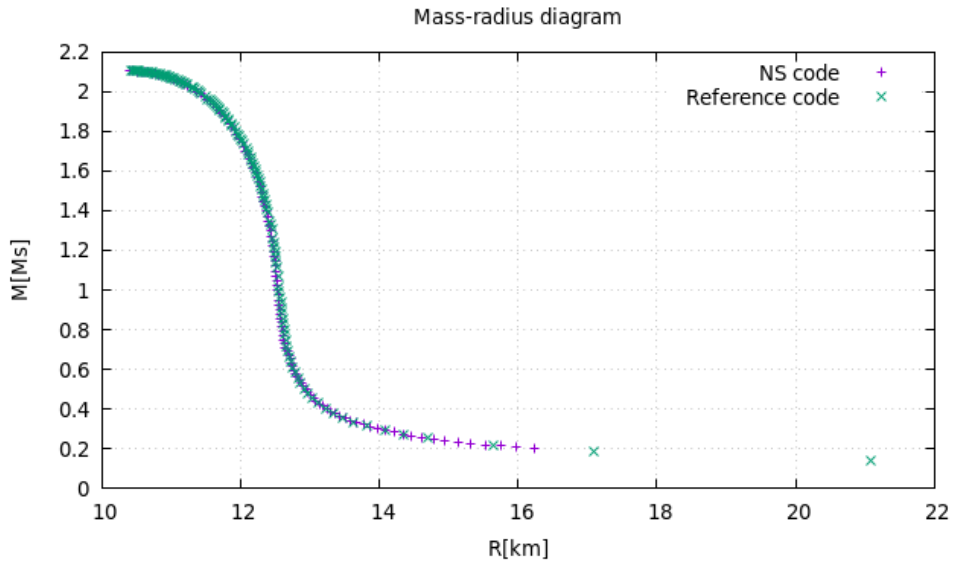

Figure 6.6: Comparison of our results (in purple) with the ones obtained with the public code developed by [6] and [2] (in green). In the diagram: mass in solar masses $M_\odot$ as function of the radius in km for neutron stars with BL equation of state.

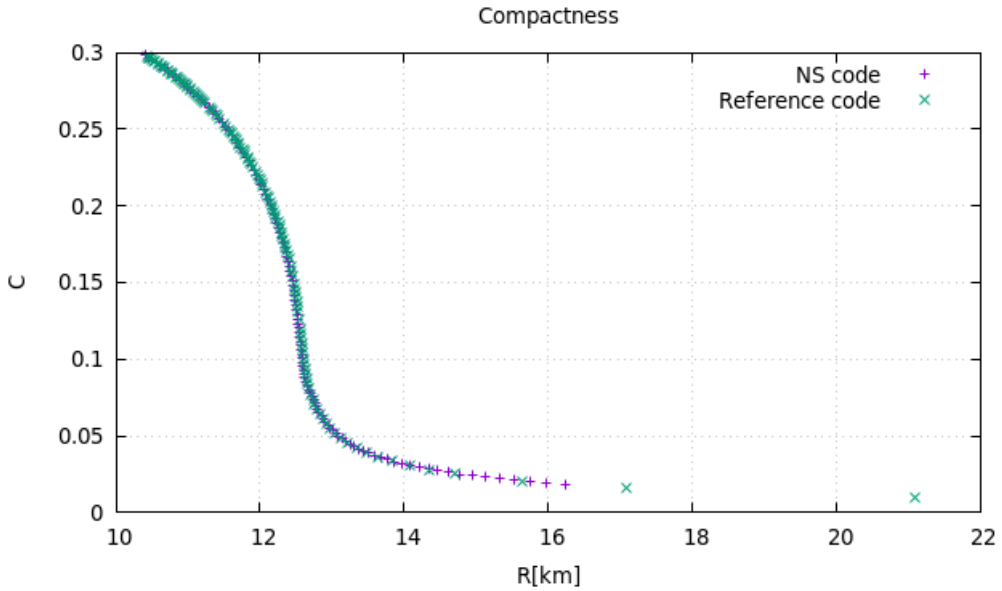

Figure 6.7: Comparison of our results (in purple) with the ones obtained with the public code developed by [6] and [2] (in green). In the diagram: compactness as function of the radius in km for neutron stars with BL equation of state.

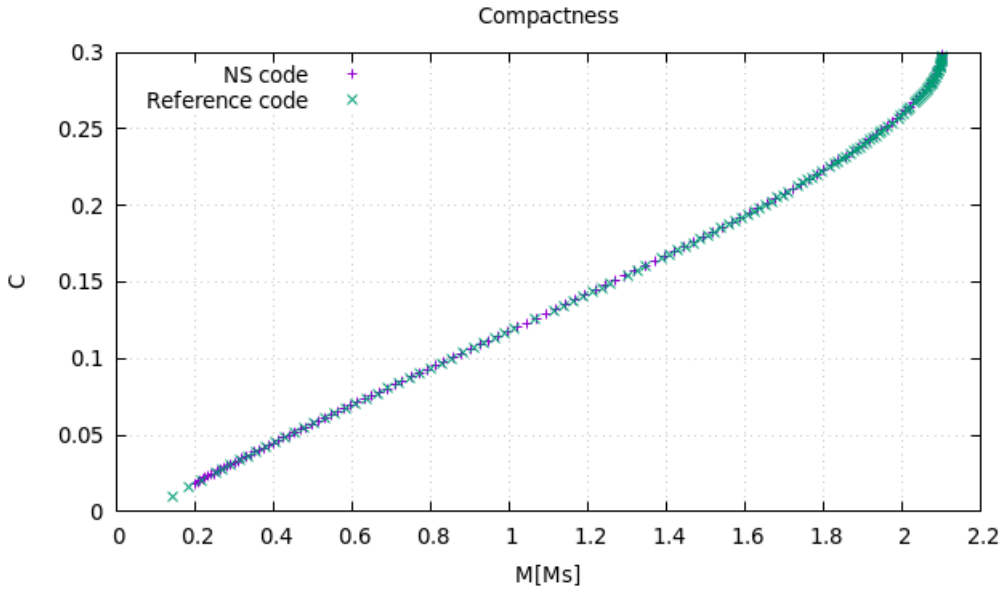

Figure 6.8: Comparison of our results (in purple) with the ones obtained with the public code developed by [6] and [2] (in green). In the diagram: compactness as function of the mass in solar masses $M_\odot$ for neutron stars with BL equation of state.

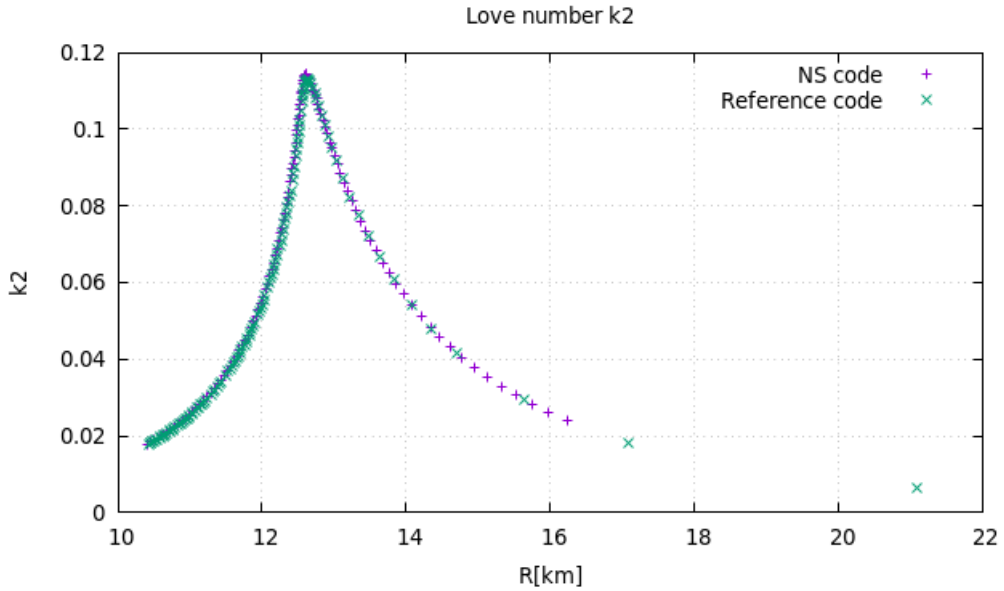

Figure 6.9: Comparison of our results (in purple) with the ones obtained with the public code developed by[6] and [2] (in green). In the diagram: Love number k_2 as function of the radius in km for neutron stars with BL equation of state.

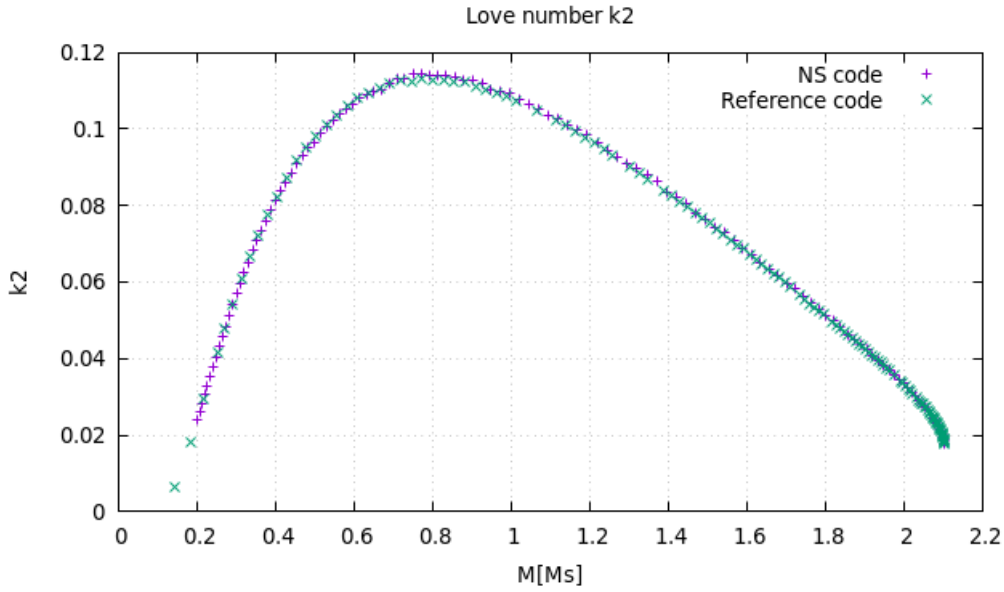

Figure 6.10: Comparison of our results (in purple) with the ones obtained with the public code developed by [6] and [2] (in green). In the diagram: Love number k_2 as function of the mass in solar masses $M_\odot$ for neutron stars with BL equation of state.

Chapter 7

Conclusions

In this final chapter we will briefly recap the topics studied in this thesis and the results obtained with our code in appendix A.1.
In chapter 2 we have introduced compact objects and in particular neutron stars and pulsars, starting from their formation in supernova explosions and their observational properties. We have discussed a model, the magnetic dipole model, that predicts that the spin-down of pulsars period $\dot{P}$ is related to the magnetic field $\dot{P} \propto B^2$ and that the magnetic field magnitude can be inferred from the measure of the period P and its time derivative, as $B \propto \sqrt{P\dot{P}}$. We have then discussed the equations that describe the structure of stars, focusing in particular on the mass equation and on the equation for the hydrostatic equilibrium, firstly from a Newtonian point of view and secondly in general relativity, introducing the Tolman-Oppenheimer-Volkoff equations.
In chapter 3 we have discussed, mainly from a qualitative point of view, the microscopic of neutron stars and some possible equations of state. The first equation of state that we have seen was the polytropic equation of state, in the non-relativistic and in the ultra-relativistic limits. This was derived from modelling the neutron star as a gas of ultra-cold ($T = 0$) fermions. Unfortunately, integrating this equation of state together with the TOV equations leads to unrealistic neutron stars models. Therefore, we have discussed a little more in details the possible matter composition of neutron stars. In our code, we have used the Bombaci-Logoteta (BL) equation of state, discussed in details in ref. [3] and [8].
In the subsequent chapter 4 we have studied binary systems and in particular binary systems of two neutron stars. Starting from the study of the dynamical evolution of binary systems in Newtonian gravity we have derived Kepler's laws and we have then discussed what happens in general relativity, where the emission of gravitational waves causes a loss of energy and momentum in a binary system with a consequent evolution of the parameters of the orbits. We have explained the equations that describe such evolution and we have seen how orbits tend to circularize during the inspiral of the two objects. We have then briefly discussed the accretion mechanism and the Hulse-Taylor binary, as archetype of double neutron stars binary systems.
In chapter 5 we have seen how in the final stages of a merger the tidal forces between the neutron stars tend to stretch them. We have therefore studied tidal forces, firstly in Newtonian gravity taking the Earth-Moon systems as example and deriving the classic tidal forces relation $\propto GM/r^3$ and secondly in general relativity. In this frame we have introduced the quadrupole moment Q_{ij} that in case of static or quasi-static perturbation can be written to linear order as $Q_{ij} = -\lambda \mathscr{E}_{ij}$, where $\mathscr{E}_{ij}$ is the quadrupole tidal field. From the coefficient λ we can define the dimensionless one $k_2 = 3G\lambda/2R^5$, which is the Love number k_2. Such coefficient is the object of our computational calculation as explained in chapter 6. In this chapter we have explained the method that we have used to integrate the TOV equations 2.22 and 2.23 together with the Love number theory equations 5.31, 5.33, 5.34 and 5.35. Firstly we have reduced the equations in dimensionless form, in order to avoid numerical errors and then we have used Runge Kutta IV order to integrate the equations, inferring the information from the tabulated equation of state

with a linear interpolation. In section 6.4 we have presented our results: the mass-radius diagram 6.1 is compatible with one of a compact object, as the mass increases with the decrease of the radius and the Love numbers k_2 obtained are in the range expected for a neutron star (between 0.05 and 0.15). Finally, in section 6.5, we have confronted our results with the ones obtained with a public code developed as explained in ref. [2] and [6] and we have seen, in figures 6.6, 6.7, 6.8, 6.9 and 6.10 that the two results are compatible.

Appendix A

Appendix

A.1 Neutron star code

Code written in C and described in chapter 6 to compute the mass-radius diagram and the Love number k_2 of a neutron star with BL equation of state. Note that in the following text, the hook arrows indicates the continuation of the previous line.

```
/*:
COMPUTATION OF THE MASS-RADIUS DIAGRAM AND THE LOVE NUMBER K2 FOR A NEUTRON STAR WITH BL
    ↪ EQUATION OF STATE
*/

//Libraries
#include <stdio.h>
#include <math.h>
#include <stdlib.h>

//def pi
#define PI 3.141592653589

//Dimensionless quantity
double r; //radius (integration variable)
double p; //pressure at distance r from the centre of the star
double *pPtr=&p; //pressure poynter
double m; //mass enclosed in a shell of radius r
double *mPtr=&m; // mass poynter
double y; //function to integrate for the calculation of Love number k2
double *yPtr=&y; //y function poynter
double eps(double p); // function that returns the energy density at a given pressure
double depsdp(double p); //function that returns the derivative of energy density respect to
    ↪ pressure at a given pressure

/*
Integration method: Runge-Kutta IV order
dp/dr=f(r,p,m,y)
dm/dr=g(r,p,m,y)
dy/dr=u(r,p,m,y)
NB: f and g are given by TOV equations, u given by Love coefficient's theory
*/

//declaration of function's parameters
double fargs[]={};
double *fargsPtr=&fargs[0];
double gargs[]={};
double *gargsPtr=&gargs[0];
double uargs[]={};
```

```
double *uargsPtr=&uargs[0];

//declaration of functions
double f(double r, double p, double m, double y, double *fargPtr);
double g(double r, double p, double m, double y, double *gargsPtr);
double u(double r, double p, double m, double y, double *uargsPtr);


//declaration of Runge-Kutta IV order method
int RK4(double r, double *pPtr, double *mPtr, double *yPtr, double h, double(*f)(double, double,
    ↪  double, double, double*), double(*g)(double, double, double, double, double*), double(*u
    ↪ )(double, double, double, double, double*));

//declaration of functions that enter in the calculation of y
double F(double r, double mcorr, double pcorr, double ycorr);
double Q(double r, double mcorr, double pcorr, double ycorr);

//declaration of function that calculates the love coefficient of a star
double love(double C, double YR);

//declaration of functions and arrays for the input of the EOS
#define LENGTH 200 //lenght of arrays pressure and energy (from EOS)
double pressure_array[LENGTH];
double log_pressure_array[LENGTH];
double energy_array[LENGTH];
double log_energy_array[LENGTH];

int read_pressure();
int read_energy();


int main(){

       //read of file in input (pressure and energy density)
       read_pressure();
       read_energy();

       //dimensional parameters
       double c=299792458; // [m/s]
       double G=6.6725e-11; // [Nm^2/kg]
       double Ms=1.989e30; // [kg] Solar mass
       double r0=10000.0; // [m]
       double m0=c*c*r0/G; //[kg]
       double eps0=m0*c*c/(r0*r0*r0); //[J/m^3]
       double p0=eps0; //[J/m^3]

       //Integration parameters
       double h=1e-3; //integration step
       double minimun=1e-17; // minimum to controll when p\simeq 0

       //File of output
       FILE * NSptr;
       NSptr=fopen("NS_output.txt", "w");

       //Print
       fprintf(NSptr, "#Pc[J/m^3]␣\t␣\t␣R[km]␣\t␣\t␣M[Ms]␣\t␣\t␣\t␣C␣\t␣\t␣\t␣Y(R)␣\t␣\t␣\t␣k2␣\
           ↪ n");

       for(int n=0; n<=120; n++){ // cycle that vary the boundary conditions
              //boundary condition (at the center of the star)
              r=0.0; // radius at the center of the star
```

```
            m=0.0; // mass at the center of the star
            p=1e-1/(pow(1.05, n)); //variation of the central pressure at every cycle
            y=2.0; //boundary condition y function

            fprintf(NSptr, "%10.8e␣\t", p*p0); //print

            //variables to save final value of parameters
            double rf=0;
            double pf=0;
            double mf=0;
            double yf=0;

            //Integration
            while(p>minimun){
                    r=r+h; //step
                    rf=r;
                    pf=p;
                    mf=m;
                    yf=y;
                    RK4(r, pPtr, mPtr, yPtr, h, f, g, u); //integration step on p, m, y
            }

            //Results extrapolation
            double R=rf*r0*1e-3; //Radius in km
            double M=mf*m0/Ms; //Mass in Solar masses
            double YR=yf; //Y value at the radius star R
            double C=mf/rf; //Compactness
            double k2=love(C, YR); //Love number k2

            //Print of results
            fprintf(NSptr, "%10.8e␣\t␣%10.8e␣\t␣%10.8e␣\t␣%10.8e␣\t␣%10.8e␣\n", R, M, C, YR,
                ↪ k2);
    }

    //file closure
    fclose(NSptr);

return 0;
}

//def Runge-Kutta IV: makes a step h of integration
int RK4(double r, double *pPtr, double *mPtr, double *yPtr, double h, double(*f)(double, double,
    ↪  double, double, double*), double(*g)(double, double, double, double, double*), double(*u
    ↪ )(double, double, double, double, double*)){
    //corrent variables
    double pcorr=*pPtr;
    double mcorr=*mPtr;
    double ycorr=*yPtr;
    //first step of the method
    double k1=h*f(r, pcorr, mcorr, ycorr, fargsPtr);
    double l1=h*g(r, pcorr, mcorr, ycorr, gargsPtr);
    double d1=h*u(r, pcorr, mcorr, ycorr, uargsPtr);
    //second step of the method
    double k2=h*f(r+h/2, pcorr+k1/2, mcorr+l1/2, ycorr+d1/2, fargsPtr);
    double l2=h*g(r+h/2, pcorr+k1/2, mcorr+l1/2, ycorr+d1/2, gargsPtr);
    double d2=h*u(r+h/2, pcorr+k1/2, mcorr+l1/2, ycorr+d1/2, uargsPtr);
    //third step of the method
    double k3=h*f(r+h/2, pcorr+k2/2, mcorr+l2/2, ycorr+d2/2, fargsPtr);
    double l3=h*g(r+h/2, pcorr+k2/2, mcorr+l2/2, ycorr+d2/2, gargsPtr);
    double d3=h*u(r+h/2, pcorr+k2/2, mcorr+l2/2, ycorr+d2/2, uargsPtr);
    //fourth step of the method
```

```
        double k4=h*f(r+h, pcorr+k3, mcorr+l3, ycorr+d3, fargsPtr);
        double l4=h*g(r+h, pcorr+k3, mcorr+l3, ycorr+d3, gargsPtr);
        double d4=h*u(r+h, pcorr+k3, mcorr+l3, ycorr+d3, uargsPtr);

        //Calculation of p(r+h), m(r+h), y(r+h)
        *pPtr=pcorr+(k1+2*k2+2*k3+k4)/6.0;
        *mPtr=mcorr+(l1+2*l2+2*l3+l4)/6.0;
        *yPtr=ycorr+(d1+2*d2+2*d3+d4)/6.0;
return 0;
}


//def of functions that enter in RK4: from TOV and Love number's theory

double f(double rl, double pl, double ml, double yl, double *fargsPtr){
        double out=0;
        out=-(pl+eps(pl))*(ml+4.0*PI*rl*rl*rl*pl)/(rl*rl-2.0*ml*rl);
return out;
}

double g(double rl, double pl, double ml, double yl, double *gargsPtr){
        double out=0;
        out=4.0*PI*rl*rl*eps(pl);
return out;
}

double u(double rl, double pl, double ml, double yl, double *uargsPtr){
        double out=0;
        out=-yl*yl/(rl)-F(rl, pl, ml, yl)*yl/(rl)-rl*Q(rl, pl, ml, yl);
return out;
}


//def of function eps: gives the energy density at a given pressure (from linear interpolation
    ↪ of EOS)
double eps(double pl){
        double out=0;

//Linear interpolation
        double logpl=log10(pl);
        int nn=0;
        if(logpl<log_pressure_array[0]){
                printf("WARNING:␣pressure␣value␣to␣low␣%10.8e␣\t␣%10.8e\n", logpl,
                    ↪ log_pressure_array[0]);
                nn=0;
        }
        if(logpl>log_pressure_array[LENGTH-1]){
                printf("WARNING:␣pressure␣value␣to␣high␣%10.8e␣\t␣%10.8e\n", logpl,
                    ↪ log_pressure_array[LENGTH-1]);
                nn=LENGTH-2;
        }

        while(((logpl<log_pressure_array[nn])||(logpl>log_pressure_array[nn+1]))){
                nn++;
        }
        double alpha=(logpl-log_pressure_array[nn])/(log_pressure_array[nn+1]-log_pressure_array[
            ↪ nn]);
        out=log_energy_array[nn]*(1-alpha)+alpha*log_energy_array[nn+1];
        out=pow(10.0, out);
return out;
}
```

```
//def of the derivative of energy density repsect to pressure at a given pressure (from linear
    ↪ interpolation of EOS)
double depsdp(double pl){
       double out=0;

//Linear interpolation
       double logpl=log10(pl);
       int nn=0;
       if(logpl<log_pressure_array[0]){
              printf("WARNING:␣pressure␣value␣to␣low␣\n");
              nn=0;
       }
       if(logpl>log_pressure_array[LENGTH-1]){
              printf("WARNING:␣pressure␣value␣to␣high␣\n");
              nn=LENGTH-2;
       }
       while(((logpl<log_pressure_array[nn])||(logpl>log_pressure_array[nn+1]))){
              nn++;
       }
       out=(energy_array[nn+1]-energy_array[nn])/(pressure_array[nn+1]-pressure_array[nn]);
return out;
}


//def of functions F and Q that enters in the calculation of y

double F(double rl, double pcorr, double mcorr, double ycorr){
       double out=0;
       out=(rl-4.0*PI*rl*rl*rl*(eps(pcorr)-pcorr))/(rl-2.0*mcorr);
return out;
}

double Q(double rl, double pcorr, double mcorr, double ycorr){
       double out=0;
       out=4.0*PI*rl*(5.0*eps(pcorr)+9.0*pcorr+(eps(pcorr)+pcorr)*depsdp(pcorr)-6.0/(4.0*PI*rl*
           ↪ rl))/(rl-2.0*mcorr)-4.0*(mcorr+4.0*PI*pcorr*rl*rl*rl)*(mcorr+4.0*PI*pcorr*rl*rl*
           ↪ rl)/((rl*rl-2*mcorr*rl)*(rl*rl-2*mcorr*rl));
       return out;
}


//Def of Love function: give the Love number K2 of a star
double love(double C, double YR){
       double out=0;
       double out1=8.0*C*C*C*C*C/5.0*(1.0-2.0*C)*(1.0-2.0*C);
       double out2=2.0+2.0*C*(YR-1.0)-YR;
       double out3=2.0*C*(6.0-3.0*YR+3.0*C*(5.0*YR-8.0));
       double out4=4.0*C*C*C*(13.0-11.0*YR+C*(3.0*YR-2.0)+2*C*C*(1+YR));
       double out5=3.0*(1.0-2.0*C)*(1.0-2.0*C)*(2.0-YR+2.0*C*(YR-1.0))*log(1.0-2.0*C);
       out=out1*out2/(out3+out4+out5);
return out;
}

//def of the function that reads in input the pressure from EOS
int read_pressure(){
       FILE * pressurePtr;
       pressurePtr=fopen("pressure.txt", "r");
       for(int ll=0; ll<LENGTH; ll++){
              fscanf(pressurePtr, "%lf", &pressure_array[ll]);
              log_pressure_array[ll]=log10(pressure_array[ll]);
```

```
        }
        fclose(pressurePtr);
return 0;
}

//def of the function that reads in input the energy density from EOS
int read_energy(){
        FILE * energyPtr;
        energyPtr=fopen("energy.txt", "r");
        for(int ll=0; ll<LENGTH; ll++){
                fscanf(energyPtr, "%lf", &energy_array[ll]);
                log_energy_array[ll]=log10(energy_array[ll]);
        }
        fclose(energyPtr);
}
```

A.2 Neutron star code output

In the following table we report the sequence of mass, radius, compactness and Love number k_2 for neutron stars with BL equation of state, output of the code in appendix A.1.

#Pc[J/m^3]	R[km]	M[Ms]	C	Y(R)	k2
1.21058205e+35	1.04000000e+01	2.10156357e+00	2.98394732e-01	1.42179874e+00	1.78263231e-02
1.15293528e+35	1.04600000e+01	2.10125611e+00	2.96639694e-01	1.39072991e+00	1.84436457e-02
1.09803360e+35	1.05100000e+01	2.10043242e+00	2.95112739e-01	1.36057093e+00	1.90363010e-02
1.04574629e+35	1.05700000e+01	2.09907703e+00	2.93248196e-01	1.34353109e+00	1.95368747e-02
9.95948847e+34	1.06200000e+01	2.09717692e+00	2.91603353e-01	1.30790704e+00	2.02550244e-02
9.48522711e+34	1.06800000e+01	2.09472452e+00	2.89626051e-01	1.28214180e+00	2.09236028e-02
9.03354963e+34	1.07300000e+01	2.09172844e+00	2.87864121e-01	1.25835752e+00	2.15493832e-02
8.60338060e+34	1.07800000e+01	2.08818083e+00	2.86042986e-01	1.22581392e+00	2.23294176e-02
8.19369581e+34	1.08300000e+01	2.08406675e+00	2.84161429e-01	1.19250959e+00	2.31601046e-02
7.80351982e+34	1.08900000e+01	2.07937138e+00	2.81959117e-01	1.17048353e+00	2.39112406e-02
7.43192364e+34	1.09400000e+01	2.07408086e+00	2.79956349e-01	1.15109194e+00	2.46049518e-02
7.07802251e+34	1.09900000e+01	2.06818209e+00	2.77890078e-01	1.12485607e+00	2.54429202e-02
6.74097382e+34	1.10400000e+01	2.06166338e+00	2.75759602e-01	1.09466165e+00	2.63898095e-02
6.41997507e+34	1.10900000e+01	2.05451581e+00	2.73564602e-01	1.06934685e+00	2.73002182e-02
6.11426197e+34	1.11400000e+01	2.04673977e+00	2.71305999e-01	1.04879408e+00	2.81695160e-02
5.82310664e+34	1.11900000e+01	2.03835894e+00	2.68987770e-01	1.01988738e+00	2.92366462e-02
5.54581584e+34	1.12400000e+01	2.02936990e+00	2.66610263e-01	9.95020214e-01	3.02790059e-02
5.28172937e+34	1.12900000e+01	2.01976340e+00	2.64173053e-01	9.77697607e-01	3.12197187e-02
5.03021845e+34	1.13400000e+01	2.00953106e+00	2.61675841e-01	9.59289007e-01	3.22258665e-02
4.79068424e+34	1.13800000e+01	1.99866527e+00	2.59346125e-01	9.28921695e-01	3.34786556e-02
4.56255642e+34	1.14300000e+01	1.98715968e+00	2.56725197e-01	9.17842594e-01	3.44232887e-02
4.34529183e+34	1.14800000e+01	1.97500958e+00	2.54044196e-01	8.87600499e-01	3.58553478e-02
4.13837317e+34	1.15200000e+01	1.96221358e+00	2.51521872e-01	8.66559225e-01	3.70752760e-02
3.94130778e+34	1.15600000e+01	1.94878758e+00	2.48936528e-01	8.44104310e-01	3.83893747e-02
3.75362646e+34	1.16100000e+01	1.93476945e+00	2.46081497e-01	8.28512875e-01	3.96510484e-02
3.57488234e+34	1.16500000e+01	1.92016059e+00	2.43384875e-01	8.19348052e-01	4.07264766e-02
3.40464985e+34	1.16900000e+01	1.90496060e+00	2.40632036e-01	7.94953852e-01	4.22711646e-02
3.24252366e+34	1.17300000e+01	1.88916962e+00	2.37823574e-01	7.78576728e-01	4.36565087e-02
3.08811778e+34	1.17700000e+01	1.87278913e+00	2.34960240e-01	7.62066338e-01	4.51062197e-02
2.94106455e+34	1.18100000e+01	1.85582153e+00	2.32042893e-01	7.55010600e-01	4.63226154e-02
2.80101386e+34	1.18500000e+01	1.83827120e+00	2.29072625e-01	7.32413143e-01	4.80875058e-02
2.66763224e+34	1.18800000e+01	1.82014583e+00	2.26241205e-01	7.08637445e-01	4.99050050e-02
2.54060214e+34	1.19200000e+01	1.80148350e+00	2.23170092e-01	7.06095627e-01	5.11349349e-02
2.41962108e+34	1.19500000e+01	1.78232799e+00	2.20242780e-01	6.86908360e-01	5.29312180e-02
2.30440103e+34	1.19900000e+01	1.76268740e+00	2.17089129e-01	6.72115221e-01	5.47112029e-02
2.19466765e+34	1.20200000e+01	1.74257051e+00	2.14075936e-01	6.62181177e-01	5.62983896e-02
2.09015967e+34	1.20500000e+01	1.72198658e+00	2.11020514e-01	6.44593608e-01	5.82506795e-02
1.99062825e+34	1.20800000e+01	1.70094570e+00	2.07924409e-01	6.42302123e-01	5.96436888e-02
1.89583643e+34	1.21100000e+01	1.67945887e+00	2.04789265e-01	6.29877931e-01	6.15114787e-02
1.80555851e+34	1.21400000e+01	1.65753875e+00	2.01616914e-01	6.18297600e-01	6.34094856e-02
1.71957953e+34	1.21700000e+01	1.63520158e+00	1.98409599e-01	6.17681433e-01	6.48679547e-02
1.63769479e+34	1.21900000e+01	1.61250641e+00	1.95334837e-01	6.02877938e-01	6.69604538e-02
1.55970932e+34	1.22200000e+01	1.58949327e+00	1.92074383e-01	5.98638685e-01	6.86808755e-02
1.48543745e+34	1.22400000e+01	1.56617704e+00	1.88947607e-01	5.86589638e-01	7.07667130e-02
1.41470233e+34	1.22600000e+01	1.54257311e+00	1.85796379e-01	5.76826060e-01	7.28002439e-02
1.34733556e+34	1.22800000e+01	1.51869706e+00	1.82622694e-01	5.82623319e-01	7.40517888e-02
1.28317672e+34	1.23100000e+01	1.49456479e+00	1.79282812e-01	5.73105887e-01	7.62402475e-02
1.22207307e+34	1.23200000e+01	1.47019274e+00	1.76216076e-01	5.67980243e-01	7.80899531e-02
1.16387911e+34	1.23400000e+01	1.44559805e+00	1.72987353e-01	5.58371917e-01	8.03246010e-02
1.10845630e+34	1.23600000e+01	1.42080323e+00	1.69745169e-01	5.58149812e-01	8.20467484e-02
1.05567266e+34	1.23800000e+01	1.39587468e+00	1.66497511e-01	5.63598443e-01	8.34377752e-02
1.00540254e+34	1.23900000e+01	1.37084587e+00	1.63380147e-01	5.44735550e-01	8.63293718e-02
9.57526226e+33	1.24100000e+01	1.34573446e+00	1.60128838e-01	5.48907953e-01	8.78511326e-02
9.11929739e+33	1.24200000e+01	1.32055779e+00	1.57006552e-01	5.44635586e-01	8.98841081e-02
8.68504513e+33	1.24400000e+01	1.29533308e+00	1.53759882e-01	5.57930397e-01	9.07928354e-02
8.27147155e+33	1.24500000e+01	1.27007718e+00	1.50640838e-01	5.54526271e-01	9.28002844e-02
7.87759195e+33	1.24600000e+01	1.24480703e+00	1.47525111e-01	5.57718902e-01	9.43533904e-02
7.50246853e+33	1.24700000e+01	1.21953957e+00	1.44414700e-01	5.54602696e-01	9.63864272e-02
7.14520812e+33	1.24800000e+01	1.19429742e+00	1.41312268e-01	5.53935576e-01	9.82572433e-02

#Pc[J/m^3]	R[km]	M[Ms]	C	Y(R)	k2
6.80496012e+33	1.24900000e+01	1.16914087e+00	1.38224925e-01	5.59271431e-01	9.96669351e-02
6.48091440e+33	1.25000000e+01	1.14409578e+00	1.35155689e-01	5.65771582e-01	1.00972357e-01
6.17229942e+33	1.25100000e+01	1.11917761e+00	1.32106341e-01	5.67993438e-01	1.02614061e-01
5.87838040e+33	1.25200000e+01	1.09440087e+00	1.29078545e-01	5.78566970e-01	1.03551273e-01
5.59845753e+33	1.25200000e+01	1.06977978e+00	1.26174622e-01	5.77658924e-01	1.05378813e-01
5.33186431e+33	1.25300000e+01	1.04532769e+00	1.23192237e-01	5.86683008e-01	1.06405256e-01
5.07796601e+33	1.25400000e+01	1.02105765e+00	1.20236046e-01	5.94611847e-01	1.07499358e-01
4.83615811e+33	1.25400000e+01	9.96982245e-01	1.17401014e-01	5.94599585e-01	1.09228905e-01
4.60586486e+33	1.25500000e+01	9.73118201e-01	1.14499563e-01	6.08967176e-01	1.09686110e-01
4.38653797e+33	1.25600000e+01	9.49511414e-01	1.11632978e-01	6.21274439e-01	1.10284528e-01
4.17765520e+33	1.25600000e+01	9.26179705e-01	1.08889895e-01	6.20449817e-01	1.12032216e-01
3.97871924e+33	1.25700000e+01	9.03132800e-01	1.06095826e-01	6.30782301e-01	1.12745671e-01
3.78925642e+33	1.25800000e+01	8.80379695e-01	1.03340685e-01	6.46515700e-01	1.12885656e-01
3.60881564e+33	1.25800000e+01	8.57928639e-01	1.00705336e-01	6.57918718e-01	1.13349312e-01
3.43696728e+33	1.25900000e+01	8.35787133e-01	9.80283992e-02	6.69025316e-01	1.13844800e-01
3.27330217e+33	1.26000000e+01	8.13962139e-01	9.53928049e-02	6.82439847e-01	1.14058018e-01
3.11743064e+33	1.26100000e+01	7.92459958e-01	9.27991931e-02	6.96576980e-01	1.14143660e-01
2.96898156e+33	1.26100000e+01	7.71288723e-01	9.03199846e-02	7.06947738e-01	1.14524255e-01
2.82760148e+33	1.26200000e+01	7.50477135e-01	8.78132538e-02	7.23182742e-01	1.14283430e-01
2.69295379e+33	1.26400000e+01	7.30035328e-01	8.52861997e-02	7.48733136e-01	1.13035295e-01
2.56471790e+33	1.26500000e+01	7.09966785e-01	8.28761305e-02	7.61756114e-01	1.13005679e-01
2.44258848e+33	1.26900000e+01	6.90274124e-01	8.03233719e-02	7.87604676e-01	1.11651583e-01
2.32627474e+33	1.27100000e+01	6.70959580e-01	7.79529881e-02	8.12860007e-01	1.10215808e-01
2.21549975e+33	1.27200000e+01	6.52024657e-01	7.56935490e-02	8.27520503e-01	1.09822598e-01
2.10999976e+33	1.27400000e+01	6.33470340e-01	7.34241313e-02	8.45102485e-01	1.09087707e-01
2.00952358e+33	1.27600000e+01	6.15297076e-01	7.12059256e-02	8.65483497e-01	1.07987558e-01
1.91383198e+33	1.27800000e+01	5.97505600e-01	6.90387765e-02	8.91335504e-01	1.06227191e-01
1.82269713e+33	1.28000000e+01	5.80108666e-01	6.69239156e-02	9.09932863e-01	1.05200808e-01
1.73590203e+33	1.28200000e+01	5.63110091e-01	6.48615384e-02	9.29021874e-01	1.04064037e-01
1.65324003e+33	1.28500000e+01	5.46508110e-01	6.28022846e-02	9.53090584e-01	1.02343569e-01
1.57451431e+33	1.28800000e+01	5.30300641e-01	6.07978538e-02	9.77309703e-01	1.00548646e-01
1.49953744e+33	1.29100000e+01	5.14485026e-01	5.88475595e-02	1.00013813e+00	9.88526040e-02
1.42813089e+33	1.29400000e+01	4.99058352e-01	5.69506928e-02	1.02824241e+00	9.65200660e-02
1.36012466e+33	1.29700000e+01	4.84017389e-01	5.51065153e-02	1.04689308e+00	9.51845446e-02
1.29535682e+33	1.30100000e+01	4.69358436e-01	5.32732621e-02	1.07424778e+00	9.28531820e-02
1.23367316e+33	1.30500000e+01	4.55077797e-01	5.14940553e-02	1.09872291e+00	9.07942516e-02
1.17492682e+33	1.30900000e+01	4.41176318e-01	4.97684946e-02	1.12478736e+00	8.85157293e-02
1.11897792e+33	1.31400000e+01	4.27652778e-01	4.80593499e-02	1.15184485e+00	8.60989126e-02
1.06569326e+33	1.31900000e+01	4.14502318e-01	4.64049306e-02	1.17794326e+00	8.37482101e-02
1.01494596e+33	1.32500000e+01	4.01719918e-01	4.47702425e-02	1.20622120e+00	8.11316552e-02
9.66615203e+32	1.33100000e+01	3.89300387e-01	4.31905505e-02	1.23231869e+00	7.87192021e-02
9.20585907e+32	1.33700000e+01	3.77238286e-01	4.16645136e-02	1.26002810e+00	7.60986988e-02
8.76748483e+32	1.34400000e+01	3.65528184e-01	4.01609114e-02	1.28957837e+00	7.32574241e-02
8.34998555e+32	1.35100000e+01	3.54164465e-01	3.87107508e-02	1.31424506e+00	7.09185354e-02
7.95236719e+32	1.35900000e+01	3.43141377e-01	3.72851240e-02	1.34274795e+00	6.81459537e-02
7.57368304e+32	1.36800000e+01	3.32453137e-01	3.58861029e-02	1.37303050e+00	6.51662006e-02
7.21303147e+32	1.37700000e+01	3.22093967e-01	3.45406582e-02	1.40135977e+00	6.23767208e-02
6.86955378e+32	1.38700000e+01	3.12057947e-01	3.32231453e-02	1.42890079e+00	5.96575303e-02
6.54243217e+32	1.39700000e+01	3.02339037e-01	3.19580137e-02	1.45585618e+00	5.69842019e-02
6.23088778e+32	1.40900000e+01	2.92931250e-01	3.06998795e-02	1.48619615e+00	5.39468565e-02
5.93417884e+32	1.42100000e+01	2.83828579e-01	2.94947015e-02	1.51234227e+00	5.13380909e-02
5.65159890e+32	1.43400000e+01	2.75025000e-01	2.83207651e-02	1.54116700e+00	4.84416618e-02
5.38247514e+32	1.44700000e+01	2.66514483e-01	2.71978292e-02	1.56768817e+00	4.57768286e-02
5.12616680e+32	1.46200000e+01	2.58291003e-01	2.60881850e-02	1.59394155e+00	4.31348784e-02
4.88206362e+32	1.47800000e+01	2.50346050e-01	2.50119913e-02	1.62100196e+00	4.04054016e-02
4.64958440e+32	1.49500000e+01	2.42670560e-01	2.39694384e-02	1.64590106e+00	3.78930316e-02
4.42817562e+32	1.51300000e+01	2.35258789e-01	2.29608990e-02	1.67124402e+00	3.53322602e-02
4.21731011e+32	1.53200000e+01	2.28105075e-01	2.19866034e-02	1.69504066e+00	3.29256193e-02
4.01648582e+32	1.55300000e+01	2.21203848e-01	2.10330949e-02	1.71905907e+00	3.04946873e-02
3.82522459e+32	1.57500000e+01	2.14549559e-01	2.01154164e-02	1.74138688e+00	2.82320029e-02
3.64307104e+32	1.59800000e+01	2.08136723e-01	1.92333041e-02	1.76208220e+00	2.61309633e-02
3.46959147e+32	1.62300000e+01	2.01959926e-01	1.83750548e-02	1.78352852e+00	2.39541194e-02

Bibliography

[1] Paul D Beale and RK Pathria. *Statistical Mechanics*. 2011.

[2] Sebastiano Bernuzzi and Alessandro Nagar. "Gravitational waves from pulsations of neutron stars described by realistic Equations of State". In: *Phys. Rev.* D78 (2008), p. 024024. DOI: 10.1103/PhysRevD.78.024024. arXiv: 0803.3804 [gr-qc].

[3] Ignazio Bombaci and Domenico Logoteta. "Equation of state of dense nuclear matter and neutron star structure from nuclear chiral interactions". In: *Astronomy & Astrophysics* 609 (2018), A128.

[4] Bradley W Carroll and Dale A Ostlie. *An introduction to modern astrophysics*. Cambridge University Press, 2017.

[5] James J Condon and Scott M Ransom. *Essential radio astronomy*. Vol. 2. Princeton University Press, 2016.

[6] Thibault Damour and Alessandro Nagar. "Relativistic tidal properties of neutron stars". In: *Phys. Rev.* D80 (2009), p. 084035. DOI: 10.1103/PhysRevD.80.084035. arXiv: 0906.0096 [gr-qc].

[7] Tanja Hinderer. "Tidal Love numbers of neutron stars". In: *The Astrophysical Journal* 677.2 (2008), p. 1216.

[8] Domenico Logoteta, Albino Perego, and Ignazio Bombaci. "Microscopic equation of state of hot nuclear matter for numerical relativity simulations". In: *Astronomy & Astrophysics* 646 (2021), A55.

[9] Malcolm S Longair. *High energy astrophysics*. Cambridge university press, 2010.

[10] Duncan R Lorimer. "Binary and millisecond pulsars". In: *Living reviews in relativity* 11.1 (2008), pp. 1–90.

[11] Michele Maggiore. *Gravitational waves: Volume 1: Theory and experiments*. OUP Oxford, 2007.

[12] Michele Maggiore. *Gravitational Waves: Volume 2: Astrophysics and Cosmology*. Oxford University Press, 2018.

[13] Tuhin Malik et al. "GW170817: Constraining the nuclear matter equation of state from the neutron star tidal deformability". In: *Physical Review C* 98.3 (2018), p. 035804.

[14] Charles W Misner, Kip S Thorne, and John Archibald Wheeler. *Gravitation*. Macmillan, 1973.

[15] Stephan Rosswog and Marcus Bruggen. *Introduction to high-energy astrophysics*. 2003, p. 376.

[16] Stuart L Shapiro and Saul A Teukolsky. *Black holes, white dwarfs, and neutron stars: The physics of compact objects*. John Wiley & Sons, 2008.

[17] TM Tauris and EPJ Van Den Heuvel. "Formation and evolution of compact stellar X-ray sources". In: *Cambridge Astrophysics Series* 39 (2006), p. 623.

[18] Joel M Weisberg, David J Nice, and Joseph H Taylor. "Timing measurements of the relativistic binary pulsar PSR B1913+ 16". In: *The Astrophysical Journal* 722.2 (2010), p. 1030.